Biomaterials 32 (2011) 1950–1956

Contents lists available at ScienceDirect

Biomaterials

journal homepage: www.elsevier.com/locate/biomaterials

A scalable controlled-release device for transscleral drug delivery to the retina

Takeaki Kawashima [a,1], Nobuhiro Nagai [b,1], Hirokazu Kaji [a,c], Norihiro Kumasaka [b], Hideyuki Onami [d], Yumi Ishikawa [b], Noriko Osumi [e], Matsuhiko Nishizawa [a,c], Toshiaki Abe [b,*]

[a] Department of Bioengineering and Robotics, Graduate School of Engineering, Tohoku University, 6-6-01 Aramaki-Aoba, Aoba-ku, Sendai 980-8579, Japan
[b] Division of Clinical Cell Therapy, Center for Advanced Medical Research and Development, ART, Tohoku University Graduate School of Medicine, 2-1 Seiryo-machi, Aoba-ku, Sendai 980-8575, Japan
[c] JST, CREST, Sanbancho, Chiyoda-ku, Tokyo 102-0075, Japan
[d] Department of Ophthalmology, Tohoku University Graduate School of Medicine, 1-1 Seiryo-machi, Aoba-ku, Sendai 980-8574, Japan
[e] Division of Developmental Neuroscience, Center for Neuroscience, ART, Tohoku University Graduate School of Medicine, 2-1 Seiryo-machi, Aoba-ku, Sendai 980-8575, Japan

ARTICLE INFO

Article history:
Received 13 October 2010
Accepted 3 November 2010
Available online 26 November 2010

Keywords:
Drug-delivery system
Transscleral delivery
Controlled release
Retinal neuroprotection
Polyethylene glycol

ABSTRACT

A transscleral drug-delivery device, designed for the administration of protein-type drugs, that consists of a drug reservoir covered with a controlled-release membrane was manufactured and tested. The controlled-release membrane is made of photopolymerized polyethylene glycol dimethacrylate (PEGDM) that contains interconnected collagen microparticles (COLs), which are the routes for drug permeation. The results showed that the release of 40-kDa FITC-dextran (FD40) was dependent on the COL concentration, which indicated that FD40 travelled through the membrane-embedded COLs. Additionally, the sustained-release drug formulations, FD40-loaded COLs and FD40-loaded COLs pelletized with PEGDM, fine-tuned the release of FD40. Capsules filled with COLs that contained recombinant human brain-derived neurotrophic factor (rhBDNF) released bioactive rhBDNF in a manner dependent on the membrane COL concentration, as was found for FD40 release. When capsules were sutured onto sclerae of rabbit eyes, FD40 was found to spread to the retinal pigment epithelium. Implantation of the device was easy, and it did not damage the eye tissues. In conclusion, our capsule is easily modified to accommodate different release rates for protein-type drugs by altering the membrane COL composition and/or drug formulation and can be implanted and removed with minor surgery. The device thus has great potential as a conduit for continuous, controlled drug release.

1. Introduction

The design of drug-delivery systems targeting the retina is a most challenging ophthalmological task. The principal delivery route currently in use is topical eye drop administration, but it delivers only low drug levels to the retina, and systemic drug delivery, e.g., intravenous delivery of Cytovene, a ganciclovir-type antiviral agent for cytomegalovirus [1], can produce toxic side effects. Although intravitreal delivery allows for high concentrations of a drug to be delivered directly to the retina, the necessary surgical procedure often requires repeated injections that can cause cataracts, retinal detachment, infection, and/or vitreous hemorrhage [2]. Therefore, transscleral delivery has emerged as a more attractive method for treating retinal disorders because it can deliver a drug locally and is less invasive [3,4]. Because of its large surface area and high degree of hydration, the sclera is permeable to drugs of different sizes (up to ~70 kDa) [5]. Transscleral drug-delivery systems that range in size from microparticles to polymeric implants have been tested [6]. However, most of these systems are made of biodegradable polymers. Drug release profiles for biodegradable devices generally have a tri-phasic release profile, i.e., an initial burst, a diffusional release phase, and a final burst [7]. This complex profile occurs because the polymers erode with time and, by doing so, affect drug dissolution. Thus, a non-biodegradable device that contains a drug reservoir sealed with a semipermeable membrane allows for sustained release and reduces the sizes of the bursts [8].

Neuroprotection from retinal degenerative diseases by neurotrophic factor delivery to the retina remains a challenge for ophthalmology [9]. Intraocular administrations of brain-derived neurotrophic factor (BDNF) [10], ciliary neurotrophic factor [11], and basic fibroblast growth factor [12], have been shown to rescue degenerating photoreceptor cells in animals. Additionally, we have demonstrated that the implantation of genetically modified iris pigment epithelial cells that secrete BDNF to the subretinal space

* Corresponding author. Tel./fax: +81 (0) 22 717 8234.
E-mail address: toshi@oph.med.tohoku.ac.jp (T. Abe).
[1] Equal contribution to this work.

0142-9612/$ – see front matter © 2010 Elsevier Ltd. All rights reserved.
doi:10.1016/j.biomaterials.2010.11.006

protect photoreceptors against phototoxicity [13]. However, suitable devices that specifically deliver neurotrophic factors continuously to the retina and with minimal invasiveness have yet to be developed. Therefore, we aimed to develop a membrane-based capsule that is implantable on the sclera (Fig. 1A) and would prolong the controlled delivery of BDNF or other protein-type drugs to the retina with zero-order kinetics. The designed capsule consists of two parts, a molded triethylene glycol dimethacrylate (TEGDM) reservoir to contain the drug and a new type of controlled-release membrane sealed around the top of the reservoir (Fig. 1B). TEGDM is a biomedical material that has been clinically used as a dental filler for the restoration of teeth [14]. The controlled-release membrane was produced by photopolymerizing a mixture of polyethylene glycol dimethacrylate (PEGDM) and collagen microparticles (COLs) (PEGDM/COL membrane). PEGDM has been successfully used by us [15] and several other groups [16,17] both *in vitro* and *in vivo* as a bio-inert scaffold material that can be easily molded into different substrate shapes and then annealed by UV crosslinking. The COLs are hydrogels containing a chemically crosslinked 0.8% (w/v) collagen network [18], which is permeable to molecules with molecular weights of <200 kDa. Drugs diffuse through the interconnected COLs embedded in the membrane. Additionally, the capsule can contain various formulations and dosages of a drug so that it can be used for many different biomedical applications. Herein, we report the fabrication, characterization, and implantation on rabbit sclerae of this transscleral drug-delivery device and demonstrate its applicability for the administration of protein-type drugs to the retina.

2. Materials and methods

2.1. Fabrication of the PEGDM/COL membrane

Mixtures (900 μl) of PEGDM prepolymer (M_n 750, Aldrich), 1% 2-hydroxy-2-methylpropiophenone, and COLs at concentrations of 0, 100, 300, or 500 mg/ml were poured individually into acrylic molds (3 × 3 × 0.1 cm) and photopolymerized with UV light that had an intensity of 11.5 mJ/cm^2 for 90 s (Lightningcure LCS, Hamamtsu Photonics) to produce membranes with thicknesses of 100 μm. COLs (average diameter, 8.7 μm) were prepared as described [18]. Briefly, 10 ml of a 1% (w/v) collagen solution (Nippon Meat Packers) was emulsified in 50 ml of liquid paraffin containing 0.3% (v/v) surfactant and stirred (600 rpm) at room temperature for 5 min. To crosslink the collagen, 1 ml of 50% (v/v) water-soluble carbodiimide (Dojindo) in water was added to the emulsified mixture and stirred (600 rpm) for 1 h. Then, 50 ml of 50% (v/v) ethanol was added into the mixture and mixed for 5 min to separate the COLs from the oil phase. The mixture was centrifuged at 3000 × *g* for 5 min, and the supernatant was discarded. Ethanol (50% v/v) was mixed with the COL pellet, and then the suspension was centrifuged (3000 × *g* for 5 min). After removing the supernatant, phosphate-buffered saline (PBS) was mixed with the COL pellet and then the suspension was centrifuged (3000 × *g* for 5 min). This procedure was repeated 3 times to remove residual ethanol.

2.2. Preparation of drug formulations

Three formulations that contained the drug mimic, 40-kDa fluorescein isothiocyanate dextran (FD40) plus PBS (F_{sol}), in COLs (F_{col}), or in COLs pelletized with PEGDM (F_{pel}) were prepared. For the preparation of F_{sol}, FD40 (Sigma) was dissolved in PBS at a concentration of 10 mg/ml. For the preparation of F_{col}, PBS solutions of

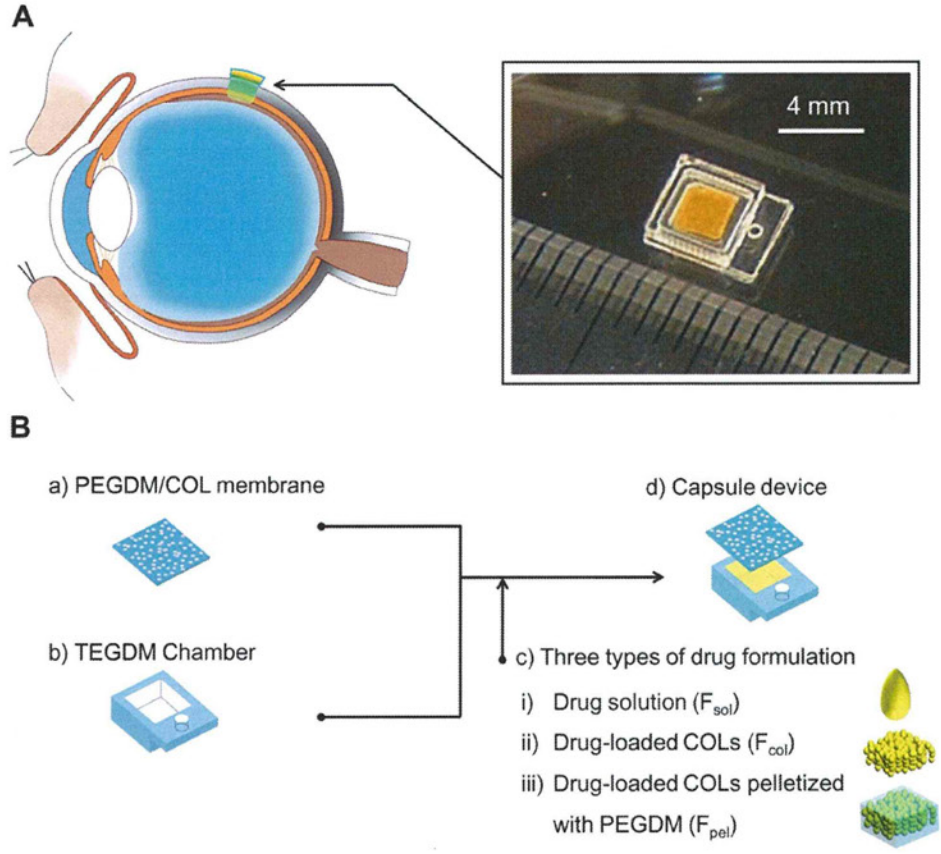

Fig. 1. (A) A transscleral drug-delivery device, designed for the administration of protein-type drugs. The photograph shows a capsule that contained FD40-loaded COLs pelletized with PEGDM and has a hole for suturing the capsule onto the sclera. (B) The capsule consists of a drug reservoir made of TEGDM and a controlled-release membrane made of photopolymerized PEGDM that contains COLs (PEGDM/COL membrane), which are the route for drug permeation. The capsule was designed so that various drug formulations could be contained in the reservoir.

COLs, which were obtained by centrifugation at 3000 × *g* for 30 min, were stirred in an equal volume of PBS that contained FD40 (20 mg/ml) for 24 h, and then the COLs were washed and centrifuged (3000 × *g* for 5 min) three times with PBS. For the preparation of F_{pel}, the FD40-loaded COLs in PBS (20 mg/ml FD40) were mixed with an equal volume of the PEGDM prepolymer and UV cured for 3 min. All drug formulations had the same amount of FD40 (10 mg/ml).

2.3. Fabrication of the capsule

A schematic of the capsule fabrication is shown in Fig. 1B. A polydimethylsiloxane master mold for the reservoir was first fabricated via a microfabrication technique that used an AutoCAD design and a micro-processing machine (Micro MC-2, PMT Co.). TEGDM prepolymer (M_w, 286.3; Aldrich) was UV cured in the mold for 3 min and peeled off to obtain a TEGDM reservoir. After loading a drug, the membrane was sealed to the reservoir by UV curing TEGDM prepolymer, which in polymerized form served as the adhesive, for 3 min.

2.4. SEM analysis

Samples were fixed with 2.5% glutaraldehyde and dehydrated first with ethanol and, subsequently, with isoamyl acetate. The samples were then dried fully in a critical point dryer (HCP-2; Hitachi Koki), coated with *Pt* using an ion coater (L350S-C; Anelva), and subjected to SEM. The SEM apparatus (VE-9800; Kyence) was operated at 5–20 kV.

2.5. In vitro release study

Modified Transwells were prepared by replacing their original porous membranes with PEGDM/COL membranes of various compositions (Fig. S2). Each drug formulation (100 μl) was placed in a Transwell and the complete systems were incubated in 400 μl of PBS at 37 °C. To estimate the amounts of FD40 that had diffused out of the Transwells, the fluorescent intensities of the PBS solutions were measured spectrofluorometrically (Fluoroscan Ascent; Thermo). For the release study that used recombinant human BDNF (rhBDNF), the capsules (reservoir interior, 5 × 5 × 2.2 mm; capsule exterior, 10 × 10 × 2.4 mm) were each filled with 40 μl of rhBDNF-loaded COLs in PBS and sealed with a membrane with a COL concentration of 0, 100, 300, or 500 mg/ml, and incubated in 1 ml of PBS at 37 °C. The amount of released rhBDNF was measured using the reagents of a BDNF-ELISA kit (Invitrogen) according to the manufacturer's instructions. Each test result is reported as the mean ± SD of three samples.

2.6. Western blotting

Immortalized retinal ganglion cells (RGC5 cells; a generous gift from Dr. N. Agarwal, University of North Texas Health Science Center, Fort Worth, TX) were maintained in Dulbecco's modified Eagle's medium (DMEM) (1 g glucose/l, Gibco) containing 10% fetal bovine serum (FBS; Gibco), L-glutamine (4 mM, Gibco), and a penicillin (100 U/ml)/streptomycin (100 mg/ml) solution (Sigma). RGC5 cells were plated into culture dishes (diameter; 60 mm, TPP) at a density of 1×10^4 cells/cm^2 and incubated in DMEM for 24 h. After starving the cells in DMEM that did not contain FBS (DMEM-f) for 12 h, the cells were exposed to conditioned DMEM-f that contained rhBDNF that had been released from a capsule into the medium (see below) or that had been spiked with rhBDNF (0, 0.1, 1, and 10 ng/ml) for 1 h. Cells were then scraped from the culture support and lysed with the reagents of a ProteoJET Cell Lysis kit (CosmoBio). Protein concentrations were determined using BCA protein assay kit reagents (Pierce). Electrophoresis was performed using 4–15% Tris-glycine gels (Biorad). Proteins were transferred to PVDF membranes using a semidry transferring system (Biorad). The membranes were blocked with 5% ECL blocking agent (GE Healthcare) and then incubated with a primary antibody against phosphorylated MAPK (1:1000; Cell Signaling) and subsequently with the secondary antibody, horseradish peroxidase-linked IgG (1:5000; Cell Signaling). After stripping the membranes of the antibodies for 10 min using the reagents of a Western Re-Probe kit (Jacksun Biotech), the membrane was probed, in a similar manner, for total MAPK (anti-MAPK antibodies, 1:1000; Cell Signaling). Bands were visualized using an enhanced chemiluminescence system (ECL Plus, GE Healthcare). Conditioned media were prepared as follows. Capsules that contained rhBDNF-loaded COLs were incubating in DMEM-f at 37 °C. The medium was replaced with fresh DMEM-f at day 3 and at week 1, 2, 3, and 4.

2.7. Implantation study

We used the eyes of six rabbits, each of which weighed between 1.8 and 2.5 kg. All animals were handled in accordance with the ARVO Statement for the Use of Animals in Ophthalmic and Vision Research after receiving approval from the Institutional Animal Care and Use Committee of the Tohoku University Environmental & Safety Committee (No.22MdA-220). The rabbits were anesthetized with ketamine hydrochloride (35 mg/kg) and xylazine hydrochloride (5 mg/kg). Their ocular surfaces were anesthetized with a topical instillation of 0.4% oxybuprocaine hydrochloride. A paralimbal conjunctival incision was made 5–8 mm from the temporal limbus. The capsules, which were loaded with F_{pel}, were sutured onto the left eyes at the sclerae with 10-0 nylon. The right eyes served as controls. At the third day of implantation, fluorescent images were captured using a handheld retinal camera for fluorescein angiography (Genesis-D, Kowa) to document the fluorescence distributions around the capsules and the sclerae. After implantation for 1 month, capsules from three rabbits were carefully removed and subjected to SEM. For histological examination, the other three rabbits were killed with an overdose of pentobarbital sodium 3 days after implantation, and their eyes were enucleated and frozen immediately in liquid nitrogen. After mounting the cryostat sections in a medium that contained 4,6-diamidino-2-phenylindole (Vectashield, Vector Lab), the distribution of FD40 was observed by fluorescent microscopy (DMI6000B, Leica).

2.8. Statistical analysis

Experimental data are presented as means ± SDs. The results were evaluated by the Student *t*-test. Differences were considered significant if $P < 0.05$.

3. Results and discussion

3.1. Device fabrication

The capsule consists of a separately fabricated PEGDM/COL membrane and a TEGDM reservoir (Fig. 1B). The membrane was prepared by UV curing a mixture of PEGDM and COLs. PEGDM is almost impermeable to macromolecules with molecular weights >40 kDa (see below); therefore, the COLs provide the route for drug permeation. Scanning electron microscopy (SEM) images were acquired to visualize the surfaces of membranes with different COL concentrations. The COLs are the round particles seen in Fig. 2A–C, and the surface density of these particles is proportional to the concentration of COLs in the corresponding unpolymerized PEGDM/COL mixture (Fig. S1). Additionally, cross-sectional SEM images showed the presence of interconnecting COLs when the COL concentration was >300 mg/ml (Fig. 2D–F). The interconnecting COLs increased in density with the concentration of the COLs. Therefore, we assumed that the drug-release rate could be controlled by changing the COL density in the membrane. Because, conventionally, semipermeable membranes are made by forming pores within the membrane i.e., solvent casting/salt leaching [19], phase separation [20], emulsion freeze-drying [21], and bubble formation [22], our method is different and therefore pioneering. For this type of membrane, there is no need to remove remaining porogens (COLs) after polymerization because the COLs act as the route for drug release.

The TEGDM reservoir was microfabricated using a polydimethylsiloxane master mold. Because photopolymerized TEGDM is impermeable to macromolecules (see below), the reservoir is a barrier that forces unidirectional drug release. After loading the drug, the membrane was placed over the reservoir and TEGDM prepolymer was UV cured along the reservoir/membrane intersection to provide a seal. Cross-sectional SEM images indicated that a tight seal was formed (Fig. 2G). The drug mimic, FD40 in PBS, did not leak from a capsule that consisted of a standard TEGDM reservoir and a PEGDM membrane that lacked COLs; therefore, the capsule had been completely sealed. The capsule was designed to contain various drug formulations and dosages. In this study, sustained-release drug formulations were encapsulated to prolong drug release by limiting the rate of drug dissolution within the reservoir (see below).

3.2. Release controllability

To demonstrate that drug release could be controlled by both the membrane and the drug formulation, modified Transwell inserts were each fitted with a membrane of defined COL concentration (Fig. S2) and loaded with one of three formulations: FD40 in PBS (F_{sol}, Fig. 3A), FD40 in COLs (F_{col}, Fig. 3B), or FD40 in COLs

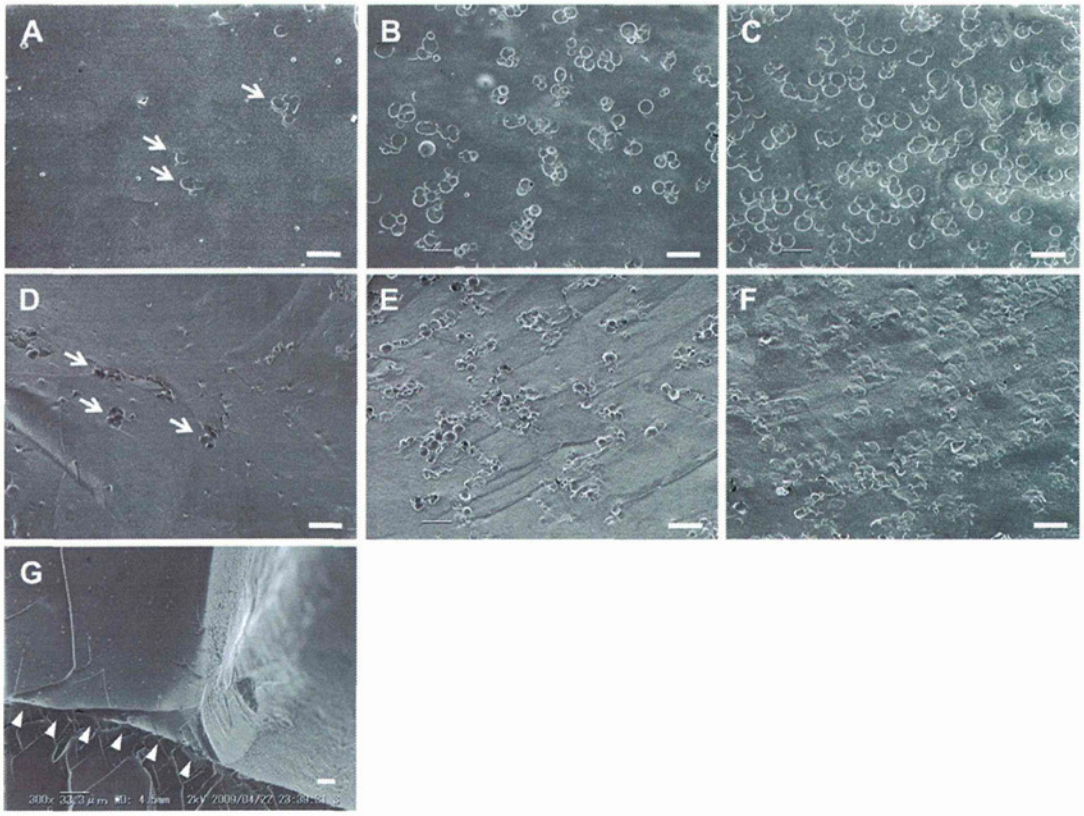

Fig. 2. Representative SEM images of (A–C) the surface and (D–F) cross sections of PEGDM/COL membranes that had COL concentrations of (A, D) 100 mg/ml, (B, E) 300 mg/ml, and (C, F) 500 mg/ml. The COLs are the round particles that form interconnecting structures throughout the membrane. Arrows point to COLs embedded in the membranes. (G) A cross-sectional SEM image of the capsule seal site that shows the formation of a tight seal. Arrowheads point to the seal site between the membrane and the capsule exterior. Bars: 20 μm.

pelletized with PEGDM (COL/PEGDM pellet) (F_{pel}, Fig. 3C). The COLs and the COL/PEGDM pellets, designed to be sustained-release drug formulations, were suspended in PBS. After placing the Transwells in PBS, FD40 release was monitored by assessing the increase in fluorescence in the external PBS solution with time. The results showed that the release of FD40 was always dependent on the COL concentration (Fig. 3A–C), which indicated that FD40 travelled through the membrane-embedded COLs. At the COL concentration of 100 mg/ml, the release kinetics was almost the same as the control (0 mg COL/ml). As shown by SEM analysis, almost no interconnected COLs existed in the 100 mg COL/ml membrane. When the membranes had been prepared with a COL concentration of 300 mg/ml, drug release followed zero-order kinetics. Additionally, F_{col} and F_{pel} behaved as sustained-release drug

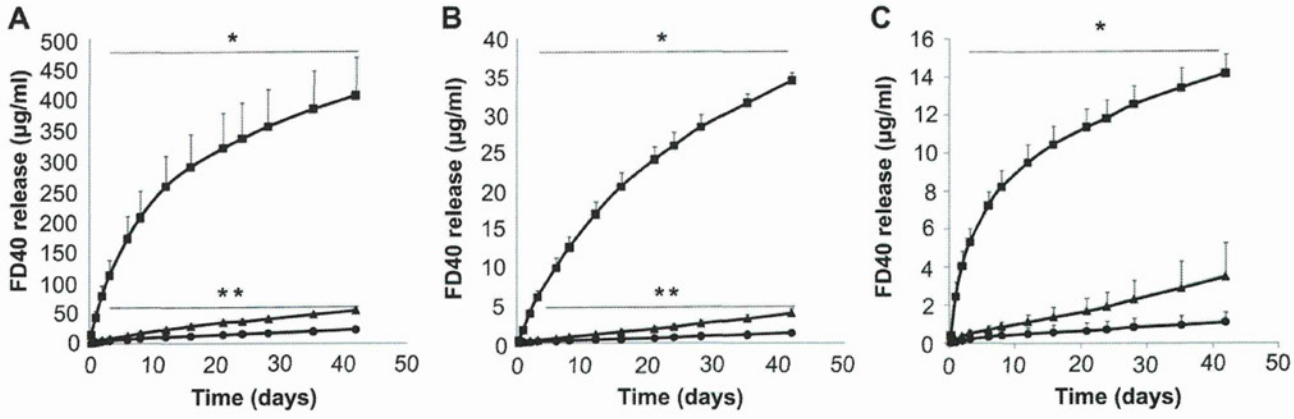

Fig. 3. Release of FD40 *in vitro*. The permeability of FD40 through PEGDM/COL membranes was studied using modified Transwells for which the PEGDM/COL membranes replaced the original Transwell membranes. The dependence of the release kinetics on the initial COL concentration for (A) FD40 in PBS (F_{sol}), (B) FD40-loaded COLs in PBS (F_{col}), and (C) FD40-loaded COLs pelletized with PEGDM in PBS (F_{pel}). The concentrations of the COLs were 100 mg/ml (circles), 300 mg/ml (triangles), and 500 mg/ml (squares). The release rate for FD40 through a membrane that did not contain COLs was almost the same as one that contained COLs at a concentration of 100 mg/ml. Error bars represent the standard deviations of three samples (error bars that are not visible are smaller than the symbols). The Means ± SDs are shown. *$P < 0.05$ for 300 mg/ml vs. 500 mg/ml **$P < 0.05$ for 100 mg/ml vs. 300 mg/ml.

formulations as they fine-tuned the release of FD40 in comparison with that of F_{sol}, perhaps because the COL and COL/PEGDM pellets, which cannot permeate the membrane, caused the reservoir solutions to have lower FD40 concentrations, which, in turn, decreased the steepness of the FD40 gradient from the reservoir to the exterior PBS solution. Therefore, the F_{col} and F_{pel} formulations, as sustained drug-release systems, improved the ability to control FD40 release by limiting the rate of FD40 dissolution, with the membrane controlling the diffusion rate via the COL tunnels. Consequently, the release of a drug can be controlled by the COL concentration in the membrane and the drug formulation.

3.3. Release mechanism

To further characterize the FD40 diffusion mechanism, we determined the diffusion coefficients for FD40 through 0.8% (w/v) crosslinked collagen (D_c), PEGDM (D_p), TEGDM (D_t), and water (D_w). D_c, D_p, and D_t were calculated using the FD40 diffusion rates through the gels (Fig. S3), and D_w was calculated using the Stokes–Einstein equation [23]. Because D_c (45.2 $\mu m^2/s$) was 1000 times larger than D_p (0.045 $\mu m^2/s$) and was smaller than D_w (67.9 $\mu m^2/s$), it appears that FD40 diffused through interconnected COLs in the membranes. If the COLs in the membrane are not interconnected, dead-ends are probably present that would inhibit the rate of drug release to the outside. However, once the COL density increases above a permeation threshold (>100 mg COL/ml), which was estimated by SEM as noted above (Fig. 2D–F), the COLs should be sufficiently interconnected that the number of dead-ends is reduced, and permeability is thereby increased. Because D_t was zero, FD40 cannot diffuse through the TEGDM reservoir, which enables unidirectional drug release.

3.4. In vitro BDNF release and bioactivity

To evaluate the release of the neurotrophic factor rhBDNF, capsules were filled with COLs that contained the protein and were tightly sealed with a membrane with a COL concentration of 0, 100, 300, or 500 mg/ml Fig. 4A presents the zero-order kinetic profiles found for rhBDNF release during a 6-week assay period. Apparently, the release kinetics of rhBDNF can be fine-tuned by varying the concentration of the COLs in a membrane in much the same manner as was found for FD40. Additionally, media that had been preincubated with capsules that contained rhBDNF induced the phosphorylation of mitogen-activated protein kinase (MAPK) in RGC5 cells when incubated with those cells as shown by western blotting of the cell extracts (Fig. 4B). BDNF is known to upregulate the expression of phosphorylated MAPK in retinal tissue [24]. In the present study, rhBDNF was found to phosphorylate MAPK in RGC5 cells in a dose-dependent manner by incubating the cells with media spiked with rhBDNF (Fig. 4C), which demonstrated that, when released from the capsule, rhBDNF retained its full activity.

Among the known neurotrophic factors, BDNF is the most potent survival factor for damaged retinal ganglion cells [10,25,26]. However, BDNF is currently administrated to the retina by intravitreal or subretinal injections in PBS [26], adenovirus vectors containing the BDNF gene [26,27], or genetically modified cells that secret BDNF [13,28]. Direct injections, however, result in extreme patient discomfort and complications arise caused by repeated injections or surgical procedures [2]. Because our capsule can contain various drug formulations, the encapsulation of the adenovirus vectors and the genetically modified cells might be possible and, as such, would represent a less invasive path than is currently available.

3.5. Implantation study

Our next challenge was to evaluate the capsule's ability to deliver a protein-type drug to the retina via the sclera. Capsules that had a reservoir (2.6 × 2.6 × 0.6 mm) filled with F_{pel} were sutured to the sclerae of three rabbits' left eyes with 10-0 nylon (Fig. 5A). The capsules abutted the sclerae but did not penetrate the conjunctivae or adjacent areas. Fig. 5B shows a fluorescent image of FD40 within a capsule, and Fig. 5C shows the release of FD40 locally at the sclera but not at the conjunctiva. This unidirectional release should reduce drug elimination by conjunctival lymphatic/blood clearance, thereby resulting in more effective delivery to the retina [29]. One month after implantation, the capsules remained sutured and neither the PEGDM of the membranes (Fig. 5D) nor the reservoirs had eroded (Fig. S4). The COLs in the membranes also survived with little biodegradation (Fig. 5D), most likely because the collagen molecules were stabilized by chemical crosslinking [18]. Although the capsules were loosely covered with connective tissue by the end of the trial, they were easily removed from the implant site. Routine ophthalmological examinations showed no eye-related toxic effects. Intense FD40 fluorescence in the sclerae adjacent to the implantation sites was observed (Fig. 5E). Furthermore, FD40 had migrated to the retinal pigment epithelium (RPE) and adjacent regions (Fig. 5F), which indicated that transscleral delivery of FD40 to the retina had been achieved. To the best of our knowledge, this is the first report that a macromolecule can be delivered to the

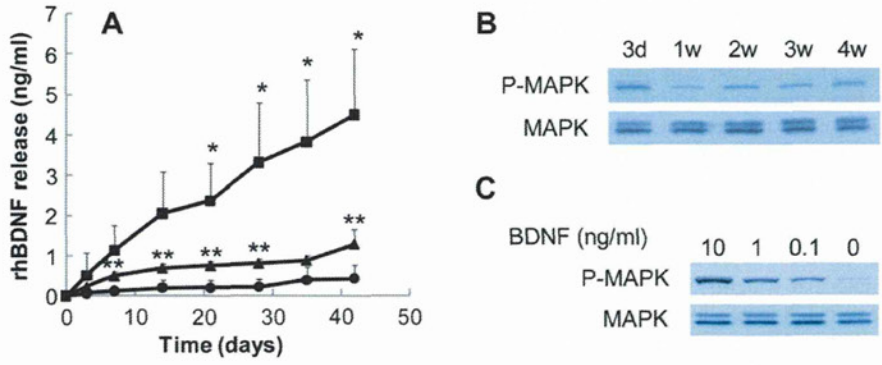

Fig. 4. Release of rhBDNF *in vitro*. (A) rhBDNF-loaded COLs in PBS were added to capsule reservoirs that sealed with a membrane with a COL concentration of 100 mg/ml (circles), 300 mg/ml (triangles), or 500 mg/ml (squares), and the release of rhBDNF was monitored using the reagents of a BDNF-ELISA kit. The release rate of rhBDNF through a PEGDM/COL membrane that contained 100 mg COL/ml was almost the same as one that contained no COLs. Means ± SDs are shown. $^*P < 0.05$ for 300 mg/ml vs. 500 mg/ml $^{**}P < 0.05$ for 100 mg/ml vs. 300 mg/ml. (B) Western blots of RGC5 cells extracts probed with antibody against phosphorylated MAPK (P-MAPK) and total MAPK. (C) The control study showed that rhBDNF could induce MAPK phosphorylation in RGC5 cells in a dose-dependent manner by incubating the cells with media spiked with rhBDNF.

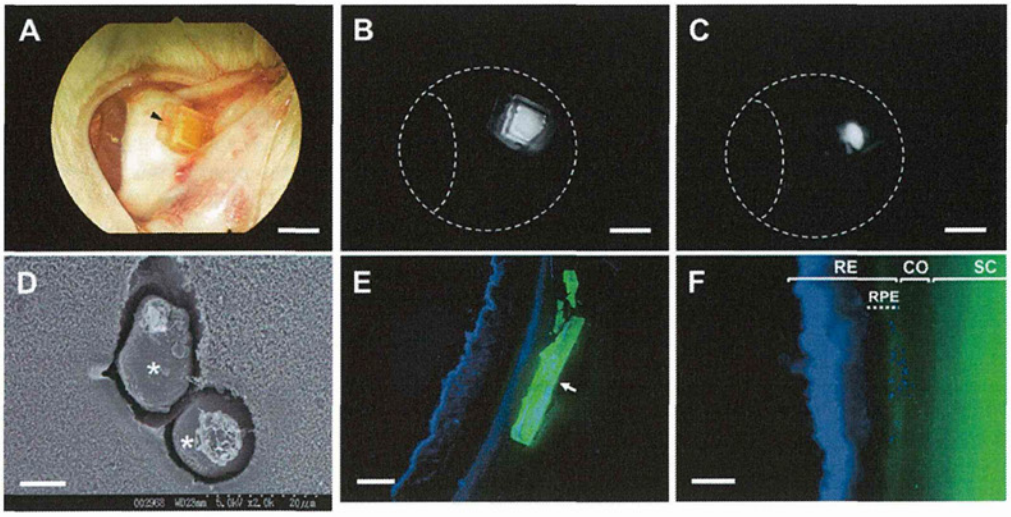

Fig. 5. Episcleral implantation of a capsule. (A) Image of a capsule sutured to the sclera of a rabbit eye 3 days after implantation. An arrowhead indicates the suture site. Fluorescent images around the sclera (B) immediately before and (C) after removal of the capsule 3 days after implantation. Fluorescence is visible as the white areas. (D) SEM image of a COL (asterisks) in the membrane of a used capsule that was removed 1 month after implantation. The COLs were not biodegraded. (E, F) The distribution of FD40 (green) in the retina and sclera around the implantation site 3 days after implantation (arrow: capsule). Cell nuclei were stained with 4,6-diamidino-2-phenylindole (blue). FD40 reached the retinal pigment epithelium. Abbreviations: sclera (SC), retinal pigment epithelium (RPE), choroid (CO), and retina (RE). Bars: 4 mm (A, B, and C), 10 μm (D), 400 μm (E), and 100 μm (F).

retina via a reservoir-based transscleral drug-delivery system, although quantification of the drug distribution still needs to be done. Proteins, as large as 50–75 kDa, penetrate into the choroid/RPE upon periocular injection [30]. Therefore, it may be possible to also deliver BDNF by the transscleral route. Given that the distribution of FD40 was somewhat concentrated at the RPE and adjacent regions, our device may be effective especially for lesions that surround the RPE. The capsule could also be used to deliver anti-angiogenic drugs, e.g., Lucentis and Macugen (for the treatment of age-related macular diseases) [31], to a lesion, e.g., the choroidal neovascular membrane, because delivery by this route will be less invasive and safer than are conventional intravitreal injections. Our non-biodegradable capsule should therefore be suitable for the transscleral delivery of protein-type drugs that require chronic suppressive-maintenance therapy over several weeks or months.

In summary, our capsule design incorporates features, outlined below, that have been absent from intraocular drug-delivery implant systems previously developed. First, the drug release kinetics can be controlled by changing the drug formulation and/or the membrane COL density so that the initial and final bursts are suppressed, which extends the release period. Second, the capsule is a scleral implantable device. To date, two ocular drug-delivery systems, Vitrasert [32] and Retisert [33], which are intravitreal sustained-release implants of ganciclovir and fluocinolone acetonide, respectively, have been marketed. Although these devices release the drugs at relatively constant rates, they must be surgically implanted in and later removed from the vitreous, which may cause complications or patient discomfort. Our capsule can be implanted and removed almost noninvasively by minor surgery. Third, most transscleral drug-delivery systems are designed to deliver low molecular weight drugs; however, ours appears able to deliver drugs of much greater molecular weights, i.e., protein-type drugs. Recent clinical trials and research have shown that many proteins are effective as drugs [9]. However, none of the available devices can deliver protein-type drugs in a controlled-release manner to the retina. Our capsule can be easily modified to accommodate different release rates for protein-type drugs by altering the membrane COL composition and/or drug formulation. Although this report demonstrated the release of only FD40 and BDNF, it should be possible to load and release low molecular weight drugs, protein-type drugs, and even drugs produced by encapsulated cells. The capsule thus has great potential for use in biomedical applications. Our future work will focus on preclinical animal studies to further assess the safety and effectiveness of the capsule.

4. Conclusion

This study reports the design and testing of a transscleral drug-delivery system that is implantable in the episclera and allows for controlled release of BDNF or other protein-type drugs with zero-order kinetics. Our microfabricated capsule consists of a drug reservoir sealed with a controlled-release membrane that contains interconnected COLs, which are the routes for drug permeation. The drug release kinetics can be controlled by changing the drug formulation and/or the membrane COL density so that the size of the bursts is reduced, which extends the release period. The capsule is designed to contain various drug formulations and dosages, allowing for a wide range of biomedical applications. The device thus has great potential as a conduit for continuous, controlled drug release.

Acknowledgments

This study was supported by the Takeda Science Foundation, the Research for Promoting Technological Seeds from the Japan Science and Technology Agency, and the Tohoku University Exploratory Research Program for Young Scientists, and was partially supported by Grants-in-Aid for Scientific Research B (20310070) and for Scientific Research on Priority Areas (21023002, 17659542, 18659508) from the Ministry of Education, Science, and Culture, Japan. Supporting information is available online or from the corresponding author.

Appendix

Figure with essential color discrimination. Fig. 4 of this article have parts that are difficult to interpret in black and white. The full

color image can be found in the online version, at doi:10.1016/j.biomaterials.2010.11.006.

Appendix. Supplementary data

Supplementary data related to this article can be found online at doi:10.1016/j.biomaterials.2010.11.006.

References

[1] Hughes PM, Olejnik O, Chang-Lin JE, Wilson CG. Topical and systemic drug delivery to the posterior segments. Adv Drug Deliv Rev 2005;57:2010–32.
[2] Geroski DH, Edelhauser HF. Transscleral drug delivery for posterior segment disease. Adv Drug Deliv Rev 2001;52:37–48.
[3] Ranta VP, Urtti A. Transscleral drug delivery to the posterior eye: prospects of pharmacokinetic modeling. Adv Drug Deliv Rev 2006;58:1164–81.
[4] Ambati J, Adamis AP. Transscleral drug delivery to the retina and choroid. Prog Retin Eye Res 2002;21:145–51.
[5] Olsen TW, Edelhauser HF, Lim JI, Geroski DH. Human scleral permeability. Effects of age, cryotherapy, transscleral diode laser, and surgical thinning. Invest Ophthalmol Vis Sci 1995;36:1893–903.
[6] Myles ME, Neumann DM, Hill JM. Recent progress in ocular drug delivery for posterior segment disease: emphasis on transscleral iontophoresis. Adv Drug Deliv Rev 2005;57:2063–79.
[7] Kunou N, Ogura Y, Yasukawa T, Kimura H, Miyamoto H, Honda Y, et al. Long-term sustained release of ganciclovir from biodegradable scleral implant for the treatment of cytomegalovirus retinitis. J Control Release 2000;68:263–71.
[8] McHugh AJ. The role of polymer membrane formation in sustained release drug delivery systems. J Control Release 2005;109:211–21.
[9] LaVail MM, Unoki K, Yasumura D, Matthes MT, Yancopoulos GD, Steinberg RH. Multiple growth factors, cytokines, and neurotrophins rescue photoreceptors from the damaging effects of constant light. Proc Natl Acad Sci U S A 1992; 89:11249–53.
[10] Di Polo A, Aigner LJ, Dunn RJ, Bray GM, Aguayo AJ. Prolonged delivery of brain-derived neurotrophic factor by adenovirus-infected Muller cells temporarily rescues injured retinal ganglion cells. Proc Natl Acad Sci U S A 1998;95:3978–83.
[11] Adamus G, Sugden B, Shiraga S, Timmers AM, Hauswirth WW. Anti-apoptotic effects of CNTF gene transfer on photoreceptor degeneration in experimental antibody-induced retinopathy. J Autoimmun 2003;21:121–9.
[12] Faktorovich EG, Steinberg RH, Yasumura D, Matthes MT, LaVail MM. Photoreceptor degeneration in inherited retinal dystrophy delayed by basic fibroblast growth factor. Nature 1990;347:83–6.
[13] Abe T, Yoshida M, Yoshioka Y, Wakusawa R, Tokita-Ishikawa Y, Seto H, et al. Iris pigment epithelial cell transplantation for degenerative retinal diseases. Prog Retin Eye Res 2007;26:302–21.
[14] Kalachandra S. Influence of fillers on the water sorption of composites. Dent Mater 1989;5:283–8.
[15] Hashimoto M, Kaji H, Nishizawa M. Selective capture of a specific cell type from mixed leucocytes in an electrode-integrated microfluidic device. Biosens Bioelectron 2009;24:2892–7.
[16] Lin-Gibson S, Bencherif S, Cooper JA, Wetzel SJ, Antonucci JM, Vogel BM, et al. Synthesis and characterization of PEG dimethacrylates and their hydrogels. Biomacromolecules 2004;5:1280–7.
[17] Weber LM, He J, Bradley B, Haskins K, Anseth KS. PEG-based hydrogels as an in vitro encapsulation platform for testing controlled beta-cell microenvironments. Acta Biomater 2006;2:1–8.
[18] Nagai N, Kumasaka N, Kawashima T, Kaji H, Nishizawa M, Abe T. Preparation and characterization of collagen microspheres for sustained release of VEGF. J Mater Sci Mater Med 2010;21:1891–8.
[19] Meier MM, Kanis LA, Soldi V. Characterization and drug-permeation profiles of microporous and dense cellulose acetate membranes: influence of plasticizer and pore forming agent. Int J Pharm 2004;278:99–110.
[20] Vogelaar L, Lammertink RG, Barsema JN, Nijdam W, Bolhuis-Versteeg LA, van Rijn CJ, et al. Phase separation micromolding: a new generic approach for microstructuring various materials. Small 2005;1:645–55.
[21] Grinberg O, Binderman I, Bahar H, Zilberman M. Highly porous bioresorbable scaffolds with controlled release of bioactive agents for tissue-regeneration applications. Acta Biomater 2010;6:1278–87.
[22] Yoon JJ, Park TG. Degradation behaviors of biodegradable macroporous scaffolds prepared by gas foaming of effervescent salts. J Biomed Mater Res 2001;55:401–8.
[23] Brandl F, Kastner F, Gschwind RM, Blunk T, Tessmar J, Gopferich A. Hydrogel-based drug delivery systems: comparison of drug diffusivity and release kinetics. J Control Release 2010;142:221–8.
[24] Klocker N, Kermer P, Weishaupt JH, Labes M, Ankerhold R, Bahr M. Brain-derived neurotrophic factor-mediated neuroprotection of adult rat retinal ganglion cells in vivo does not exclusively depend on phosphatidyl-inositol-3'-kinase/protein kinase B signaling. J Neurosci 2000;20:6962–7.
[25] Pernet V, Di Polo A. Synergistic action of brain-derived neurotrophic factor and lens injury promotes retinal ganglion cell survival, but leads to optic nerve dystrophy in vivo. Brain 2006;129:1014–26.
[26] Mansour-Robaey S, Clarke DB, Wang YC, Bray GM, Aguayo AJ. Effects of ocular injury and administration of brain-derived neurotrophic factor on survival and regrowth of axotomized retinal ganglion cells. Proc Natl Acad Sci U S A 1994;91:1632–6.
[27] Martin KR, Quigley HA, Zack DJ, Levkovitch-Verbin H, Kielczewski J, Valenta D, et al. Gene therapy with brain-derived neurotrophic factor as a protection: retinal ganglion cells in a rat glaucoma model. Invest Ophthalmol Vis Sci 2003;44:4357–65.
[28] Harper MM, Adamson L, Blits B, Bunge MB, Grozdanic SD, Sakaguchi DS. Brain-derived neurotrophic factor released from engineered mesenchymal stem cells attenuates glutamate- and hydrogen peroxide-mediated death of staurosporine-differentiated RGC-5 cells. Exp Eye Res 2009;89:538–48.
[29] Robinson MR, Lee SS, Kim H, Kim S, Lutz RJ, Galban C, et al. A rabbit model for assessing the ocular barriers to the transscleral delivery of triamcinolone acetonide. Exp Eye Res 2006;82:479–87.
[30] Demetriades AM, Deering T, Liu H, Lu L, Gehlbach P, Packer JD, et al. Transscleral delivery of antiangiogenic proteins. J Ocul Pharmacol Ther 2008;24: 70–9.
[31] Wong TY, Liew G, Mitchell P. Clinical update: new treatments for age-related macular degeneration. Lancet 2007;370:204–6.
[32] Sanborn GE, Anand R, Torti RE, Nightingale SD, Cal SX, Yates B, et al. Sustained-release ganciclovir therapy for treatment of cytomegalovirus retinitis. Use of an intravitreal device. Arch Ophthalmol 1992;110:188–95.
[33] Jaffe GJ, Martin D, Callanan D, Pearson PA, Levy B, Comstock T. Fluocinolone acetonide implant (Retisert) for noninfectious posterior uveitis: thirty-four-week results of a multicenter randomized clinical study. Ophthalmology 2006;113:1020–7.

REDUCTION OF LASER-INDUCED CHOROIDAL NEOVASCULARIZATION BY INTRAVITREAL VASOHIBIN-1 IN MONKEY EYES

HIDEYUKI ONAMI, MD,*† NOBUHIRO NAGAI, PHD,* SHIGEKI MACHIDA, MD,‡ NORIHIRO KUMASAKA, MS,* RYOSUKE WAKUSAWA, MD,† YUMI ISHIKAWA, MS,* HIKARU SONODA, PHD,§ YASUFUMI SATO, MD,¶ TOSHIAKI ABE, MD*

Purpose: To determine whether intravitreal vasohibin-1 will reduce the grade of the choroidal neovascularization in monkey eyes.

Methods: Choroidal neovascularizations were induced in 12 monkey eyes by laser photocoagulation. Three monkeys were evaluated for the safety of the vasohibin-1 injections, 6 monkeys for the effects of a single injection, and 3 monkeys for repeated injections of vasohibin-1. Ophthalmoscopy, fluorescein angiography, focal electroretinograms, and optical coherence tomography were used for the evaluations. The level of vascular endothelial growth factor in the aqueous was determined by enzyme-linked immunosorbent assay. Immunohistochemistry was performed.

Results: An intravitreal injection of 10 μg of vasohibin-1 induced mild intraocular inflammation. Eyes with an intravitreal injection of 0.1 μg and 1.0 μg of vasohibin-1 had significant less fluorescein leakage from the choroidal neovascularizations and larger amplitude focal electroretinograms than that of vehicle-injected eyes. Similar results were obtained by repeated injections of 0.1 μg of vasohibin-1. Immunohistochemistry showed that vasohibin-1 was expressed mainly in the endothelial cells within the choroidal neovascularizations. The vascular endothelial growth factor level was not significantly altered by intravitreal vasohibin-1.

Conclusion: The reduction of the laser-induced choroidal neovascularizations and preservation of macular function in monkey by intravitreal vasohibin-1 suggest that it should be considered for suppressing choroidal neovascularizations in humans.

RETINA X:1–10, 2012

Age-related macular degeneration (AMD) is one of the most common sight-threatening disease in developed countries.[1] A choroidal neovascularization (CNV) is a typical finding in eyes with the wet-type AMD, and the CNV can lead to subretinal hemorrhages, exudative lesions, serous retinal detachment, and disciform scars.[2] Many different types of treatments have been used to treat AMD, for example, laser photocoagulation,[3] surgery,[4,5] transpupillary thermotherapy,[6] photodynamic therapy,[7] and intravitreal injection of anti–vascular endothelial growth factor (VEGF).[8,9] Each of these treatments has advantages and disadvantages, and the best treatment of AMD has still not been determined.

Different pro- and antiangiogenic factors play important roles in the development and progression of CNVs.[10] Among the proangiogenic factors, VEGF has been shown to play a major role.[11] Thus, anti-VEGF therapy is being used to successfully treat CNVs in patients with AMD.[8,9] However, this method requires repeated injections that can lead to irritation, infection, and other adverse side effects.[12] In addition, not all patients respond to the therapy.[13] Thus, other types of therapy need to be developed to treat AMD eyes with a CNV.

Vasohibin-1 is a VEGF-inducible molecule expressed by human cultured endothelial cells (ECs) and has antiangiogenic properties.[14] Its expression is selectively induced in ECs not only by VEGF but also by several other proangiogenic factors such as basic fibroblast growth factor.[15] Vasohibin-1 inhibits the formation of EC networks in vitro, corneal neovascularization,[14] and retinal neovascularization in a mouse model of oxygen-induced ischemic retinopathy.[16] Vasohibin-1 is found in the vitreous and in

proliferative membranes of patients with diabetic retinopathy. The level of vasohibin-1 is significantly correlated with the VEGF level in the vitreous of patients with proliferative diabetic retinopathy.[17] Vasohibin-1 is also expressed in the CNV membranes of patients with AMD.[18] Eyes with lower vasohibin-1/VEGF expression ratios tend to have larger CNV lesions, whereas those with higher vasohibin-1/VEGF ratios have subretinal fibrosislike lesions.[18]

We have found that the laser-induced CNVs were less active in mice injected intravitreally with vasohibin-1 than those injected with the vehicle.[19] Thus, the purpose of this study was to determine the effect of intravitreal vasohibin-1 on the laser-induced CNVs in monkey eyes. We shall show that the intravitreal vasohibin-1 was safe and reduced the degree of the CNVs in monkey eyes.

Methods

Animals

The procedures used in the animal experiments followed the guidelines of the The Association for Research in Vision and Ophthalmology Statement for the Use of Animals in Ophthalmic and Vision Research, and they were approved by the Animal Care Committee of Tohoku University Graduate School of Medicine. Twelve Japanese macaque monkeys (*Macaca fuscata*) between ages 4 and 6 years and weighing between 4.2 kg and 10.1 kg were used (Table 1). For all procedures, the monkeys were anesthetized with an intramuscular injection of ketamine hydrochloride (35 mg/kg) and xylazine hydrochloride (5 mg/kg), and the pupils were dilated with topical 2.5% phenylephrine and 1% tropicamide. Oxybuprocaine hydrochloride (0.4%) was also used for local anesthesia. Three monkeys were used to evaluate the safety of intravitreal vasohibin-1, 6 monkeys for dose dependency of a single injection of vasohibin-1, and 3 monkeys for repeated injections of vasohibin-1.

Table 1. Monkey Eyes Used in This Study

	Vasohibin (mg)	Number of Eyes	Inflammation
Nontreated	0	1	0/1
	0.01	1	0/1
	0.1	1	0/1
	1	1	0/1
	10	1	1/1
	100	1	1/1
Laser application	0	3	0/3
	0.01	3	0/3
	0.1	3	0/3
	1	3	1/3
Laser application	0	3	0/3
	0.1	3	0/3
Total		24	3/24

Inflammation shows clinical inflammation signs that were observed during the experiments.

Experimental Choroidal Neovascularization

An argon green laser was used to rupture of the choroidal membrane using a slit-lamp delivery system (Ultima 2000SE; Lumenis, Yokneam, Israel) with a contact lens.[20] The laser settings were as follows: 50-μm diameter, 0.1-second duration, and 650-mW to 750-mW intensity. Five laser burns were made around the macula within 15° of the fovea. The foveola was not treated. Each burn was confirmed to have induced subretinal bubbles indicating a rupture of Bruch membrane.

Expression and Purification of Human Vasohibin-1 Polypeptide

Human vasohibin-1 was purified from *Escherichia coli* as described.[21] Human vasohibin-1 was isolated as a thioredoxin fusion protein. The fusion protein was dialyzed and digested with blood coagulation Factor Xa (Novagen, Darmstadf, Germany). The released vasohibin-1 was collected, eluted, and dialyzed against 20 mM glycine–HCl buffer (pH 3.5). Then, the vasohibin-1 was resolubilized with 50 mM Tris–HCl buffer containing 50 mM NaCl, 5 mM tris(2-carboxyethyl)phosphine, 0.5 mM ethylenediaminetetraacetic acid, 5% glycerol, and 4.4% *N*-lauroylsarcosine (pH 8.0) and was dialyzed against 20 mM sodium phosphate buffer at pH 8.0. This buffer was also used as the vehicle.

The protein concentration was determined by the Bradford method with a protein assay kit (Bio-Rad Laboratories, Hercules, CA), with bovine serum albumin as a standard protein.

From the *Division of Clinical Cell Therapy, United Center for Advanced Medical Research and Development; †Department of Ophthalmology and Visual Science, Graduate School of Medicine, Tohoku University, Miyagi, Japan; ‡Department of Ophthalmology, Iwate Medical University, Iwate, Japan; §Diagnostic Division, Shionogi & Co., Ltd. Osaka, Japan; and ¶Department of Vascular Biology, Institute of Development, Aging, and Cancer, Tohoku University Graduate School of Medicine, Miyagi, Japan.

Supported in part by grants from Grants-in-Aid for Scientific Research 21592214 and 20592030 (to T. Abe) from the Japan Society for the Promotion of Science, Chiyoda-ku, Tokyo, Japan and by Suzuken Memorial Foundation.

This study was performed at the Tohoku University. Monkeys were supplied by National BioResource Project for breeding and supply.

The authors declare no conflict of interest.

Reprint requests: Toshiaki Abe, MD, Division of Clinical Cell Therapy, United Center for Advanced Research and Translational Medicine (ART), Graduate School of Medicine, Tohoku University, 1-1 Seiryoumachi Aobaku Sendai, Miyagi, 980-8574 Japan; e-mail: toshi@oph.med.tohoku.ac.jp

Intravitreal Injection of Recombinant Vasohibin-1 Polypeptide

Vasohibin-1 was injected intravitreally in 3 groups of monkeys (Table 1). The first group of 6 eyes did not have a laser burn and received a single injection of vehicle, or 0.01, 0.1, 1, 10, or 100 μg of vasohibin-1/50 μL of vehicle. The second group of 12 eyes of 6 monkeys (3 eyes for each concentration) received a single injection of vehicle or 0.01, 0.1, and 1 μg of vasohibin-1/50 μL of vehicle 4 days after the laser burn. The third group of 3 eyes had 3 injections of 0.1 μg of vasohibin-1/50 μL of vehicle in the right eyes and 50 μL of vehicle in 3 fellow eyes on 0, 4, and 7 days after the laser burn. We examined the natural course of laser-induced CNVs in mice, and the CNVs were most active around Day 14 after the laser burn, and then gradually regressed, especially 28 days after laser burn. When we injected vasohibin-1 into the vitreous of mice after laser burns, we found that the injection of vasohibin-1 on Day 4 after the laser burn was most effective, followed by Days 7 and 1. Other days were less effective. In addition, immunohistochemical studies for vasohibin-1 in the mouse CNV membranes showed that the later the laser burn, the more vasohibin-1 staining was observed.[19] So we decided to do the repeated vasohibin-1 injections on 0, 4, and 7 days after the laser burn (relatively early days after laser burn).

For the intravitreal injections, the monkeys were anesthetized and pupils were dilated. The intravitreal injections were made with a 30-gauge needle attached to a 1-mL syringe. The needle was inserted through the sclera into the vitreous cavity ~1.5 mm posterior to the limbus while observing the eye with an operating microscope. The fundus was examined after the injection to confirm that the retina and lens were not damaged.

Ophthalmic Examinations

In addition to the routine ophthalmologic examinations, fluorescein angiography (FA) with an imaging system (GENESIS-Df; Kowa, Tokyo, Japan), optical coherence tomography (OCT, RS3000; NIDEK, Tokyo, Japan), and focal and full-field electroretinography (ERG) were performed on the selected days. Fluorescein angiography was performed 1, 2, and 4 weeks after the laser photocoagulation. Two retinal specialists (R.W. and T.A.) graded the angiograms in a masked way using a grading system[22]: Grade 1, no hyperfluorescence; Grade 2, hyperfluorescence without leakage; Grade 3, hyperfluorescence in the early or middle phase and leakage in the late phase; and Grade 4, bright hyperfluorescence in the transit and leakage in late phase beyond the treated areas.

The central macular thickness was determined from the macular thickness maps (3.45 mm in diameter) of the scans by OCT 4 weeks after the laser photocoagulation. The volume of the lesion was also calculated using the same program.

The pupils were maximally dilated for the ERG recordings 4 weeks after intravitreal vasohibin-1 injections. The ERGs were amplified and digitally bandpass filtered from 0.5 Hz to 500 Hz for the full-field ERGs and from 5 Hz to 500 Hz for the focal ERGs (PuREC; Mayo, Aichi, Japan). The animals were dark adapted for at least 30 minutes before the full-field ERG recordings. The light for the stimulus was obtained from light-emitting diodes (EW-102; Mayo Co., Nagoya, Japan) embedded in a contact lens electrode. The intensity and duration of the stimuli were controlled by an electronic stimulator (WLS-20; Mayo Co.). Chlorided silver plate electrodes were placed on the forehead and right ear lobe as reference and ground electrodes, respectively. The intensity of the stimulus was 1,000 cd/m^2 and the duration was 3 milliseconds.

Focal ERGs were recorded 4 weeks after the laser photocoagulation with a focal ERG system (PuREC; Mayo; ER-80; Kowa) that was integrated into an infrared fundus camera. This system was developed and described in detail by Miyake et al.[23,24] The stimulus spot was 15° in diameter and was placed on the macula by viewing the ocular fundus on a monitor. The intensity of the stimulus was 1,000 cd/m^2, and the background light was 1.5 cd/m^2. The stimulus duration was 100 milliseconds. A Burian–Allen bipolar contact lens electrode (Hansen Ophthalmic Laboratories, Iowa City, IA) was inserted into the anesthesized conjunctival sac to record the focal ERGs. A chlorided silver electrode was placed on the left ear lobe as the ground electrode. Two hundred to 300 responses were averaged at a stimulation rate of 5 Hz.

The a-waves were measured from the baseline to the trough of the first negative response, and the b-wave from the first trough to the peak of the following positive wave. The amplitudes of a-waves and b-waves from the three untreated monkeys were used as control. The number of monkeys used in this experiment was not added to the total number of monkeys.

Immunohistochemistry

Immunostaining for vasohibin-1was done on eyes with laser-induced CNVs 28 days after the laser application. From the results of CNV experiments on

mice,[19] the laser-induced CNV lesions were self-resolved >28 days after the laser burn. Thus, we decided to enucleate the eyes 28 days after the laser burn, although there may be differences between mice and monkeys. The eyes were enucleated and fixed in 4% paraformaldehyde overnight, and the anterior segment and lens were removed. The posterior segment was embedded in paraffin, and 3-μm serial sections were cut, and adjacent sections were stained with hematoxylin and eosin.

The immunohistochemical staining for vasohibin-1 was performed with the peroxidase method and for cytokeratin by the alkaline phosphatase method. Mouse monoclonal antibodies against vasohibin-1 (1:400) and mouse monoclonal anti-pan cytokeratin (1:200; Sigma-Aldrich, St. Louis, MO) were applied to the sections overnight at 4°C. Then the sections were incubated in biotin-conjugated anti-mouse immunoglobulin (Histfine SAB-PO(M) kit; Nichirei, Tokyo, Japan). The slides for vasohibin were incubated with peroxidase-conjugated streptavidin (Histfine SAB-PO(M) kit; Nichirei), and the slides for cytokeratin were incubated with alkaline phosphatase–conjugated streptavidin (Histfine; Nichirei). HistoGreen (HISTOPRIME HistoGreen substrate kit for peroxidase; Ab Cys SA) was used for the chromogen of vasohibin, and VECTOR RED (alkaline phosphatase substrate kit 1; Vector, Burlingame, CA) was used for the chromogen of cytokeratin. The slides were counterstained with hematoxylin. For control, preimmune mouse immunoglobulin G was used instead of the primary antibody.

Enzyme-Linked Immunosorbent Assay for Vascular Endothelial Growth Factor

Aqueous was collected by a 30-gauge needle from the anterior chamber of each monkey 4 weeks after the laser photocoagulation. The level of the VEGF peptide was quantified by enzyme-linked immunosorbent assay according to the manufacturer's instructions (R & D Systems, Mckinley, MN; Quantikine Human VEGF immunoassay) using 50 μL of aqueous. The intensity of the color of the reaction products was measured with a MAXline microplate reader (Molecular Devices Corporation, Palo Alto, CA). The measurements were made in duplicate, and the mean was used. The concentration of VEGF was expressed as the amount of protein in picograms per milliliter (pg/mL).

Statistical Analyses

Analysis of variance with Scheffe test for post hoc analysis was used to examine the differences in the leakage and intensity of the CNVs in the fluorescein angiograms, amplitudes of the ERGs, mean central thickness, and volume of the CNV. The differences were also compared using the Student two-sample *t*-tests.

Results

Safety Evaluations and Outcomes

Before any of the procedures, the retina and choroid were normal in all the monkeys. Then 6 nontreated eyes were injected intravitreally with vehicle or 0.01, 0.1, 1, 10, or 100 μg of vasohibin-1/50 μL. After 0.01, 0.1, and 1 μg of vasohibin-1, the appearance of the retina and choroid did not differ from that of the vehicle-injected eyes. When 10 μg or 100 μg/50 μL of vasohibin-1 polypeptide was injected, a mild inflammation (Grade 1)[25] was detected in the vitreous on the day after the injection. The inflammation was less with 10 μg than with 100 μg of vasohibin, and the inflammation was resolved in 2 days after 10 μg and in 1 week after 100 μg (Table 1). When we injected 1 μg/50 μL of vasohibin-1 once in the laser-treated eyes, 1 of the 3 eyes developed inflammation in the aqueous. An inflammation was not observed when 0.1 μg of vasohibin-1 was injected even after 3 injections. When we injected 50 μL of vehicle with almost the same amount of endotoxin (400 U/mL) as that of 100 μg of vasohibin-1, no inflammation was detected. These results indicated that mild inflammation can develop with $\geq$10 μg of vasohibin-1 injection into the vitreous in nontreated monkey eyes.

The amplitudes of the a- and b-waves of the full-field ERGs of eyes injected with 0.01 μg to 100 μg of vasohibin-1 did not differ significantly from the vehicle-injected eyes. The a-wave amplitudes ranged from 87.3 μV to 180.3 μV (average, 119.3 ± 36.6 μV) before and from 100.7 μV to 195.8 μV (average, 131.3 ± 53.7 μV; $P = 0.444$) after the vasohibin-1 injection. The b-wave amplitudes ranged from 219.6 μV to 340.6 μV (average 250.6 ± 54.7 μV) before and from 240.8 μV to 345.2 μV (average 274.4 ± 82.0 μV, $P = 0.801$) after the vasohibin-1 injection.

Effect of Different Concentrations of Vasohibin-1

After the laser photocoagulation, we injected vehicle or 0.01, 0.1, or 1 μg of vasohibin-1/50 μL of vehicle in 3 eyes of each dosage for a total of 12 eyes (Table 1). From the results of safety evaluations, we selected the maximum amount of vasohibin-1 as 1 μg of vasohibin-1/50 μL of vehicle. Representative results of FA at 1, 2, and 4 weeks after the laser application for each dose of vasohibin-1 are shown in Figure 1. Color fundus photographs and focal ERGs recorded at 4 weeks are also shown.

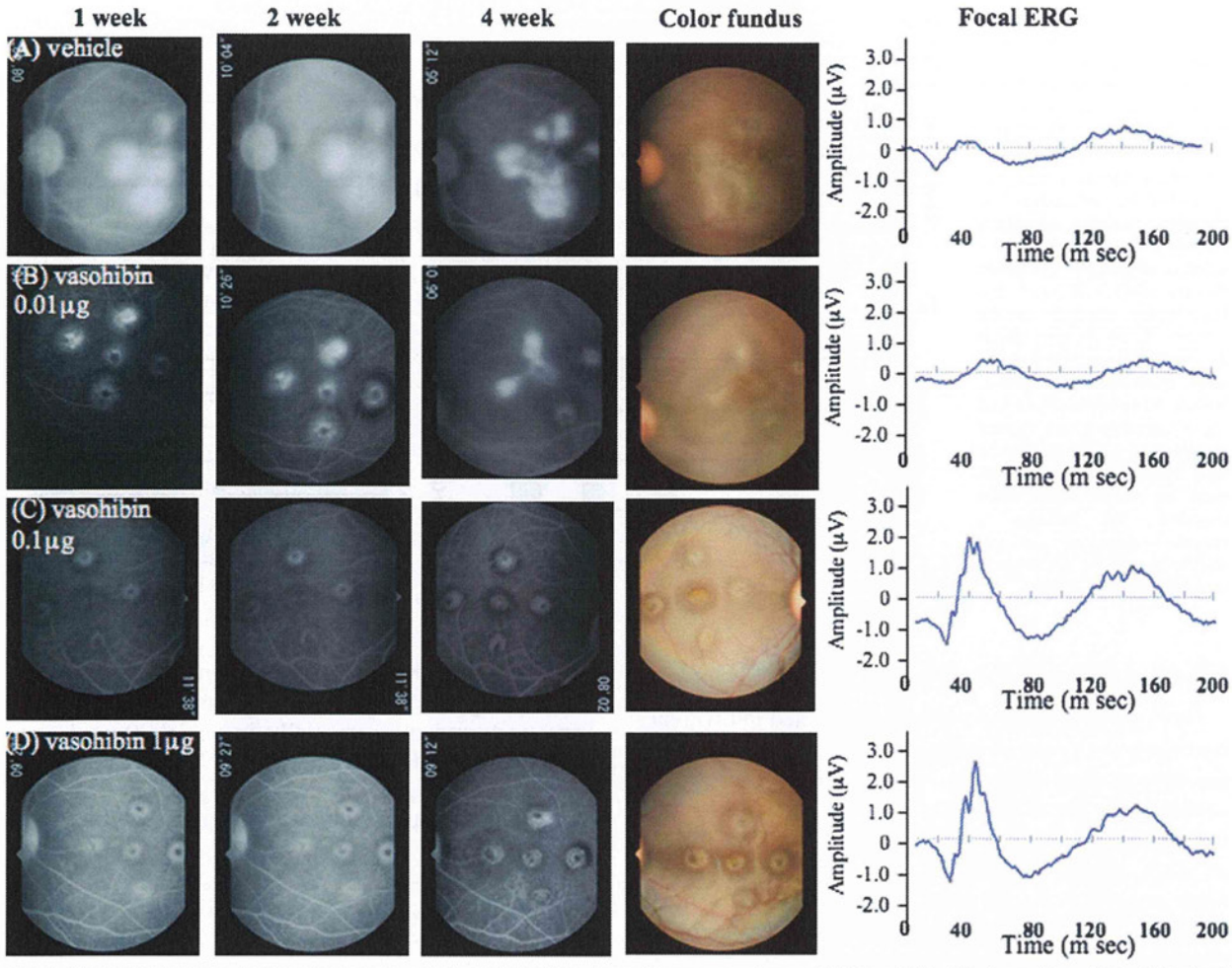

COLOR

Fig. 1. Representative FAs, fundus photographs, and focal ERGs from 6 monkey eyes are shown. Vehicle or 0.01, 0.1, 1 μg of vasohibin-1/50 μL of vehicle was injected intravitreally, and representative results at 1, 2, and 4 weeks after laser treatment are shown (see quantitative values in Figure 2, A–D). The FA images are those at around 10 minutes after the fluorescein injection. Color fundus photographs were taken 4 weeks after the laser application. Focal ERGs recorded 4 weeks after the laser photocoagulation are shown in the right column for each eye.

The CNV activity was scored using the FA grading system[22] for all five laser spots in each eye. The FA score for each spot was summed and compared with each other (Figure 2A). Our findings showed that there was significantly less leakage after 0.1 μg of vasohibin-1 than that for vehicle ($P = 0.016$) and for 0.01 μg ($P = 0.035$) of vasohibin-1 at 1 week. Significantly less leakage after 0.1 μg of vasohibin-1 than that of vehicle was also observed at 4 weeks ($P = 0.0307$). Because 1 μg of vasohibin-1 showed mild inflammation in 1 eye, we did not analyze the CNV in these eyes. The percentage of eyes with FA scores of 4 is also listed in Figure 2B. Our results showed that 45% of vehicle-treated eyes had Grade 4 leakage, and it was 45% in 0.01 μg of vasohibin-1–treated eyes, 7% with 0.1 μg of vasohibin-1–treated eyes, and none in the 1-μg vasohibin-1–treated eyes (only 2 eyes) at 1 week. Similarly, the percentage of eyes with Grade 4 leakage was 27%, 13%, 7%, and 0% at 2 weeks and 20%, 20%, 0% and 0% at 4 weeks after the vasohibin-1 injection (Figure 2B).

The amplitudes of the a-waves of the focal ERGs after 0.01 μg of vasohibin-1 were significantly smaller than those of the controls ($P = 0.041$) (Figure 2C). The amplitudes of the b-waves of the focal ERG b amplitudes in the vehicle-injected eyes ($P = 0.0085$) and in the 0.01-μg vasohibin-1–injected eye ($P = 0.0184$) were significantly smaller than those of the controls (Figure 2D). The results of inflammation, FA leakage, and ERG amplitudes led us to select 0.1 μg of vasohibin-1 as the optimal concentration for intravitreal injection to reduce the laser-induced CNV in our monkeys.

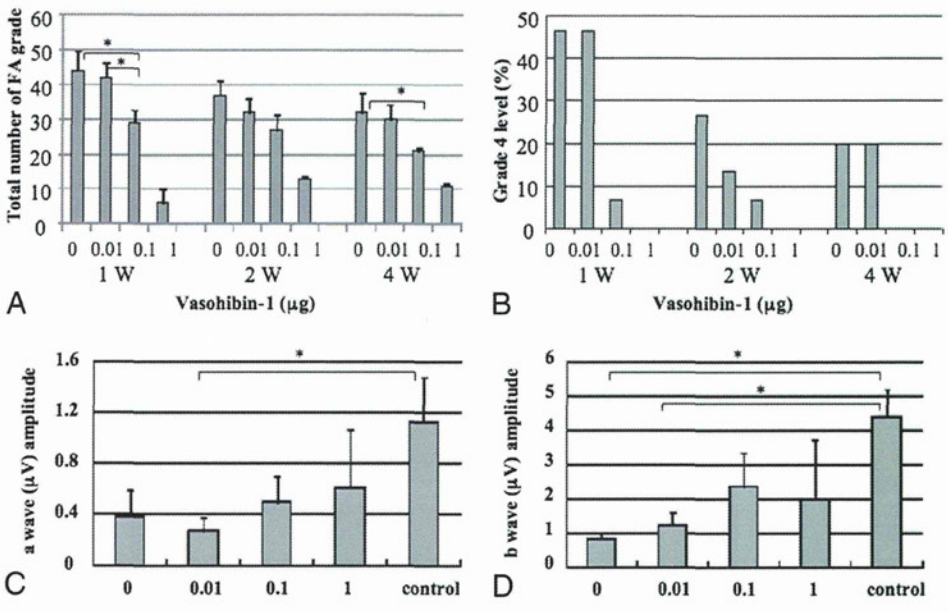

Fig. 2. Fluorescein angiographic scores for each of the 5 laser spots in each eye are plotted for each group, and the amplitudes of the a- and b-waves of the focal ERGs. **A.** Fluorescein angiographic scores for each of the five laser spots in each eye are plotted for each group. Statistically significant differences are shown as asterisks. **B.** Distribution of Grade 4 FA scores for each group is shown. **C** and **D.** Average amplitude of the a-waves (**C**) and b-waves (**D**) of the focal ERG recorded 4 weeks after intravitreal vasohibin-1. Vehicle (0) or 0.01, 0.10, or 1.00 μg of vasohibin-1 was injected in control eyes or eyes after the laser burns. Untreated controls show the effects before laser treatment. The averages ± standard deviations of the amplitudes of the a- and b-waves are plotted on the ordinate.

Effects of Repeated Injections of Vasohibin-1

Next, we examined the effects of repeated intravitreal injections of 0.1 μg of vasohibin-1/50 μL of vehicle in the right eyes on 0, 4, and 7 days after the laser application while the fellow eyes received an injection of the vehicle on the same days. We studied three eyes in each group. Representative fundus photographs, FAs, and OCT images after vehicle alone are shown in Figure 3 (A and B) and after 0.1 μg of vasohibin-1/50 μL of vehicle in Figure 3 (C and D). The FA scores were significantly lower in the vasohibin-1–injected eyes than in the vehicle-injected eyes at 4 weeks (P = 0.009; Figures 3 and 4A). At 1 week and 2 weeks after the vasohibin-1 injections, the FA scores were not significantly different (P = 0.07). The percentage of eyes scored as Grade 4 was 13.3% at 1 week, 26.7% at 2 weeks, and 26.7% at 4 weeks in the vehicle-treated eyes, whereas no Grade 4 eyes were observed in the 0.1 μg of vasohibin-1/50 μL of vehicle-treated eyes at any time (Figure 4B).

Although statistical significance was not observed in the a-wave amplitude of the focal ERGs, statistically significant larger b-wave amplitudes were observed in the vasohibin-1–treated eyes than that of vehicle (P = 0.039) (Figure 4, C and D).

Optical coherence tomography examinations showed that the retinal pigment epithelium and Bruch membrane were disrupted in the laser-treated eyes at 1 week and 2 weeks after the laser application (Figure 3, B and D) as was found in histologic preparations.[22] At 4 weeks, an retinal pigment epithelium–like membrane appeared over the CNV lesion (Figure 3, B and D). This line was shown to be cytokeratin positive. The OCT images showed that the size of the CNV increased gradually especially in vehicle-treated eyes as was seen in the FA images.

Optical coherence tomography also showed that the macular thickness (Figure 4E) and volume (Figure 4F) of the CNV lesions after 0.1 μg of vasohibin-1/50 μL of treated eyes was ~30% less than the vehicle-treated eyes in the central 1 mm. When we examined the volume of the central 6 mm, no difference was observed between the vasohibin-1–treated and vehicle-treated eyes.

Histology and Immunostaining of Choroidal Neovascularization

Histopathologic analyses showed that the retina and choroid surrounding the CNV had normal architecture in both the vehicle and vasohibin-1–treated eyes as reported.[26] The vehicle-treated eyes after the laser application showed a disruption of the Bruch membrane and retinal pigment epithelium complex, and the eyes had different degrees of fibrous tissues and vessels (Figure 5, C and E). Eyes treated with vasohibin-1 tended to have smaller CNV than that of vehicle-treated eyes.

Cytokeratin labeling demonstrated that retinal pigment epithelial cells from the edges of the wound had proliferated and covered the laser wound to different degrees. Although a disruption of the cytokeratin labeling was present in the vehicle-treated eyes (Figure 5, D and F), we could not find any significant difference from that of the vasohibin-1–injected eyes. Different

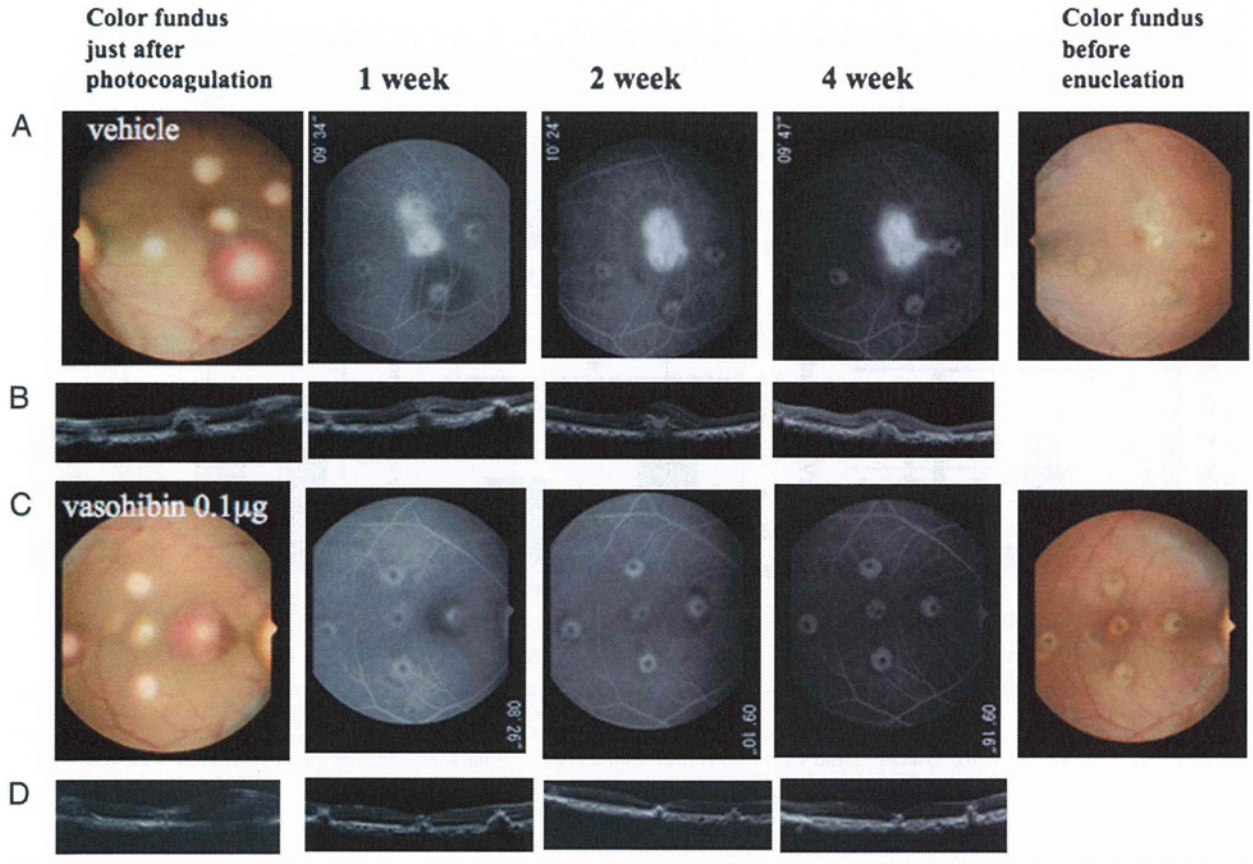

COLOR

Fig. 3. Fluorescein angiograms, ocular coherence tomographic images, color fundus photographs, and focal ERGs are shown. Vasohibin-1 (0.1 μg/50 μL) was injected into the vitreous of the right eyes 3 times on 0, 4, and 7 days after laser application, and the same amount of vehicle was injected into left eyes on the same days. Photographs show the fundus just after the laser application and the day of enucleation. Fluorescein angiographs recorded 1, 2, and 4 weeks after laser application. Photographs of the right (**A**) and left (**C**) eyes are shown. The results of OCT on the indicated days are shown in the same vertical columns for the indicated day (**B**) and (**D**).

numbers of macrophage-like cells were also observed in the neural retina.[21]

In immunostained eyes, vasohibin-1 positivity was found mainly in the CNV especially on the ECs in the CNV (Figure 5B). The regions surrounding the CNV showed little vasohibin-1–positive staining. Some monkeys showed no vasohibin-1 expression by immunohistochemistry even in the CNV at 28 day after laser application. Positive staining for vasohibin-1 appeared to be greater in the more active CNVs (Figure 5A), and it was more obvious in nontreated monkey eyes, although we could not determine whether the staining was significantly greater because only 3 monkey eyes were studied.

Vascular Endothelial Growth Factor in Aqueous During Experiments

The level of VEGF was determined by enzyme-linked immunosorbent assay. The average VEGF level in the aqueous in the vasohibin-1–injected eyes was 15.3 pg/mL, and it was 20.6 pg/mL in the vehicle-treated eyes at 4 days after laser application. The average VEGF level in the vasohibin-1– and vehicle-treated eyes were 7.0 pg/mL and 8.9 pg/mL, respectively, at 4 weeks after laser application (Figure 6). For both times, the differences were not significant.

Discussion

Our results demonstrated that when 10 μg or 100 μg of vasohibin-1 was injected intravitreally into nontreated normal monkey eyes, a mild anterior chamber inflammation developed. No signs of inflammation or any adverse effects were found when <1 μg of vasohibin-1 was injected into nonlaser treated eyes, although we used only 1 eye for each dose. However when 1 μg of vasohibin-1 was injected into laser-treated eyes, a mild inflammation developed in 1 of the 3 eyes. Inflammation has also been reported in monkey

COLOR

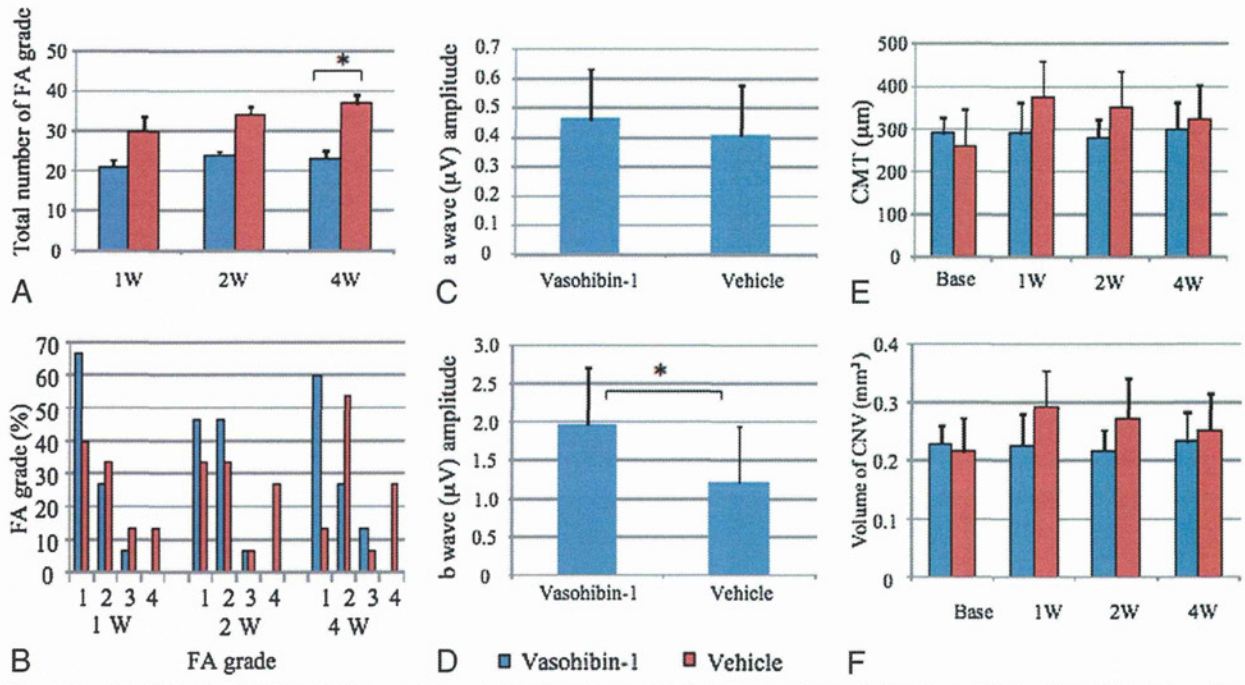

Fig. 4. Results of FA, focal ERG, and OCT are shown. **A.** Significantly less FA leakage was observed after 0.1 μg/50 μL of vasohibin-1 than after vehicle treatment at 4 weeks. **B.** Distribution of Grade 4 FA eyes for each group. **C** and **D.** Average amplitudes of the a-waves (**C**) and b-waves (**D**) of the focal ERGs. **E** and **F.** Average central macular thickness (CMT) and the central 3.4 mm and volume of area of either vasohibin-1–treated (blue) or vehicle-treated (red) eyes before (base) and 1, 2, and 4 weeks after laser application. Lower thickness and volumes were observed in the vasohibin-1–treated monkeys. Data are the standard deviations.

eyes after intravitreal injections of fragments of mouse and human chimera antibodies against VEGF.[22,27]

Fluorescein angiography examination after vasohibin-1 injection in laser-treated eyes showed significantly lower FA scores in eyes that received 0.1 μg and 1 μg of vasohibin-1 than the vehicle-injected eyes, although the number of eyes may have affected the statistics. Fluorescein leakage from the laser spots close to the macula was greater than that of the other laser spots. These results are compatible with the results of Shen et al,[28] who also found that the laser spot was larger and the leakage was greater for lesions closer to the macula. We also found that fluorescein leakage was different among monkeys, even though we applied the same amount of vasohibin-1.[22] This variability may be because the body weight ranged from 4.1 kg to 10.1 kg and age from 4 years to 6 years among the monkeys.

After we injected 0.1 μg of vasohibin-1 3 times in the right eyes and vehicle into the left eyes of 3 monkeys, we found significantly less fluorescein leakage in the vasohibin-1–treated right eyes than in the vehicle-treated eyes. The results of focal ERGs and OCT were well correlated with the results of FA findings, although the quantitative values were not significantly different.

Taken together, these results showed that intravitreal vasohibin-1 is able to reduce the activity of the laser-induced CNV in monkeys. With 3 injections of 0.1 μg of vasohibin-1, the results were not so different from that of only 1 injection at 4 days after the laser application. This may indicate that there may be an optimum time for the vasohibin-1 to affect the course of the laser-induced CNV. Alternatively, the results may be related to the half-life of vasohibin-1.

We found that vasohibin-1 was expressed on ECs especially those in the CNV lesions. Careful examinations showed that vasohibin-1 expression was limited to the CNV lesion and may not show extensive expression in other regions under normal physiologic conditions. Although we have not followed the expression of vasohibin-1 during the course of CNV development in monkeys, vasohibin-1 expression may be enhanced in the new vessels as was reported.[29] The vasohibin-1 expression appeared stronger in nontreated monkey eyes, although this could not be quantified. Vasohibin-1 has been reported to be present on the ECs only in the stroma of tumors and not in the noncancerous regions of the tissue in surgically resected tissues of the same patient.[29] These findings suggest that vasohibin-1 may be expressed mainly in the new vessels as it was in our laser-induced CNVs.

COLOR

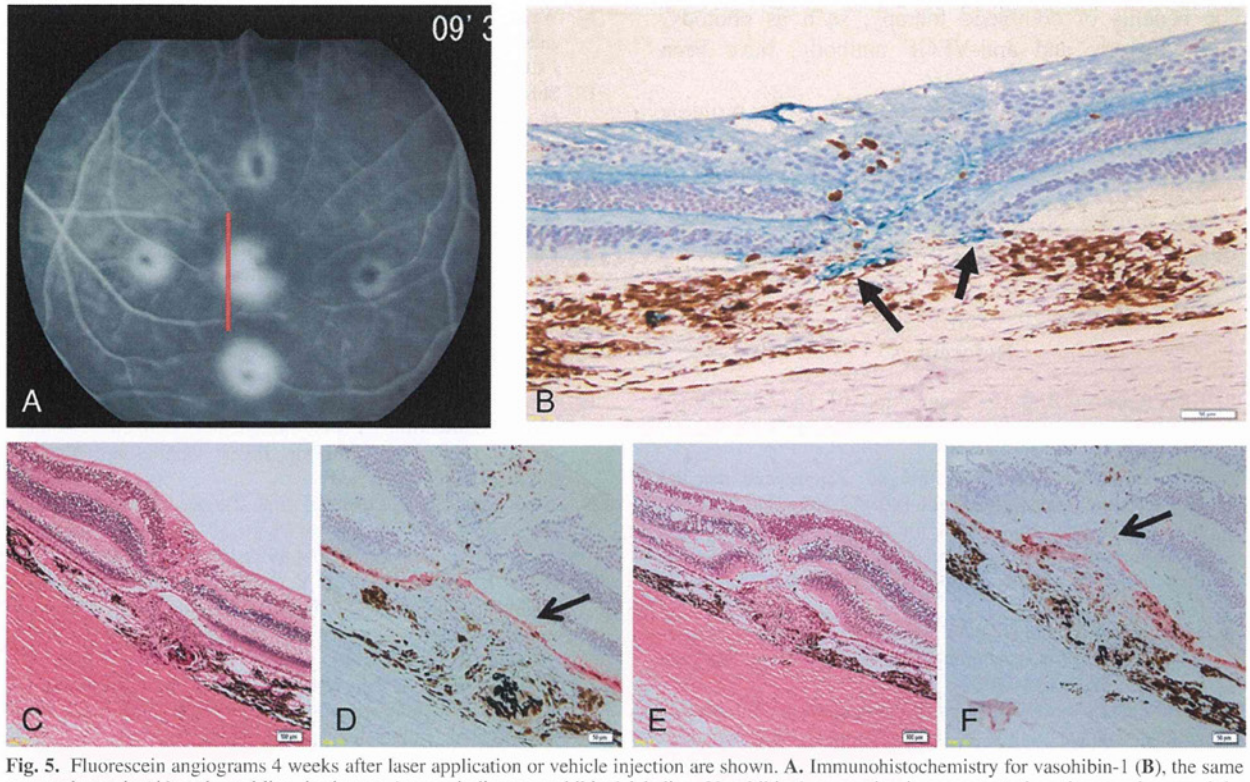

Fig. 5. Fluorescein angiograms 4 weeks after laser application or vehicle injection are shown. **A.** Immunohistochemistry for vasohibin-1 (**B**), the same eye as shown in (**A**) at the red line, is shown. Arrows indicate vasohibin-1 labeling. Vasohibin-1 expression is concentrated on the vessels around the CNV (arrows), but markedly less than in the CNV. Vaoshibin-1 expression was observed at active CNV (red line in **A**). The subretinal space is an artifact of histologic processing. Cytokeratin labeling is also shown with vasohibin-treated eye (**D**) and vehicle-treated eye (**F**). Arrows show labeling of cytokeratin. Bar = 50 μm. **C** and **E.** Hematoxylin and eosin staining of vasohibin-1–treated and vehicle-treated eyes, respectively, are shown. Bar = 100 μm. Cytokeratin labeling shows that retinal pigment epithelium covers CNV in the vasohibin-1–treated eyes (**D**), and a disruption of cytokeratin labeling is observed in vehicle-treated eye (**F**).

Hosaka et al[29] reported that exogenous vasohibin-1 blocked angiogenesis and maturation of not only the cancerous tissue but also the surrounding vessels and, thus, enhanced the antitumor effects of vasohibin-1. Intravitreal injection of vasohibin-1 may also suppress angiogenesis in CNVs by the same mechanism.

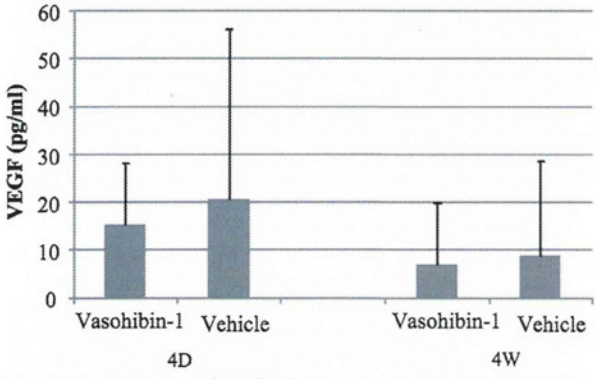

Fig. 6. Concentration of VEGF in aqueous in laser-treated monkey eyes 4 days and 4 weeks after laser application is shown. Vertical axis shows VEGF concentration in picograms per milliliter, and horizontal axis is the day of examination. Vascular endothelial growth factor in vasohibin-1–treated eyes (blue boxes) and vehicle-treated eyes (red boxes) show no significant difference at any times.

The amount of VEGF in the aqueous in the vasohibin-1–treated eyes did not differ from that in vehicle-treated eyes. Thus, Zhou et al[30] reported that external vasohibin-1 had no effect on the level of VEGF when they used adenovirus encoding human vasohibin-1 on mouse corneal neovascularization induced by alkali burn. They also reported that vasohibin-1 may downregulate the VEGF receptor 2 (VEGFR2). Shen et al[16] also reported a downregulation of VEGFR2 by vasohibin-1 during mouse ischemic retinopathy. Our previous studies have also shown a downregulation of VEGFR2 by external vasohibin-1 in laser-induced mouse CNVs.[19] Thus, vasohibin-1 may reduce the activity of a CNV by partially downregulating VEGFR2 in the eyes. If this is correct, vasohibin-1 may not affect the favorable aspects of VEGF such as its neuroprotective effect,[31] especially if VEGF works through VEGFR1 rather than VEGFR2. Vasohibin-1 also can be used with anti-VEGF antibody for CNV therapy.

The benefits of combined therapy, such as photodynamic therapy and anti-VEGF antibody, have been discussed.[27]

In conclusion, intravitreal vasohibin-1 in monkey eyes is safe and can reduce the activity of laser-induced CNVs and thus preserve the function of the macula.

Key words: choroidal neovascularization, laser-induced, monkey, vascular endothelial growth factor, vasohibin-1.

References

1. Klein R, Peto T, Bird AC, Vannewkirk MR. The epidemiology of age-related macular degeneration. Am J Ophthalmol 2004; 137:486–495.
2. Bressler NM, Bressler SB, Fine SL. Age-related macular degeneration. Surv Ophthalmol 1998;32:375–413.
3. Argon laser photocoagulation for neovascular maculopathy. Three-year results from randomized clinical trials Macular Photocoagulation Study Group. Arch Ophthalmol 1986;104: 694–701.
4. Thomas MA, Grand MG, Williams DF, et al. Surgical management of subfoveal choroidal neovascularization. Ophthalmology 1992;99:952–968.
5. Eckardt C, Eckardt U, Conrad HG. Macular rotation with and without counter-rotation of the globe in patients with age-related macular degeneration. Graefes Arch Clin Exp Ophthalmol 1999;237:313–325.
6. Reichel E, Berrocal AM, Ip M, et al. Transpupillary thermotherapy of occult subfoveal choroidal neovascularization in patients with age-related macular degeneration. Ophthalmology 1999; 106:1908–1914.
7. Photodynamic therapy of subfoveal choroidal neovascularization in age-related macular degeneration with verteporfin: one year results of 2 randomized clinical trials-TAP report Treatment of Age-related Macular Degeneration with Photodynamic Therapy (TAP). Study Group. Arch Ophthalmol 1999;117:1329–1345.
8. Grisanti S, Tatar O. The role of vascular endothelial growth factor and other endogenous interplayers in age-related macular degeneration. Prog Retin Eye Res 2008;27:372–390.
9. Miller JW, Adamis AP, Shima DT, et al. Vascular endothelial growth factor/vascular permeability factor is temporally and spatially correlated with ocular angiogenesis in a primate model. Am J Pathol 1994;145:574–584.
10. Krzystolik MG, Afshari MA, Adamis AP, et al. Prevention of experimental choroidal neovascularization with intravitreal anti-vascular endothelial growth factor antibody fragment. Arch Ophthalmol 2002;120:338–346.
11. Rosenfeld PJ, Brown DM, Heier JS, et al. Ranibizumab for neovascular age-related macular degeneration. N Engl J Med 2006;355:1419–1431.
12. Pilli S, Kotsolis A, Spaide RF, et al. Endophthalmitis associated with intravitreal anti-vascular endothelial growth factor therapy injections in an office setting. Am J Ophthalmol 2008;145:879–882.
13. Lux A, Llacer H, Heussen FMA, Joussen AM. Non-responders to bevacizumab (Avastin) therapy of choroidal neovascular lesions. Am J Ophthalmol 2007:91:1318–1322.
14. Watanabe K, Hasegawa Y, Yamashita H, et al. Vasohibin as an endothelium-derived negative feedback regulator of angiogenesis. J Clin Invest 2004;114:898–907.
15. Shimizu K, Watanabe K, Yamashita H, et al. Gene regulation of a novel angiogenesis inhibitor, vasohibin, in endothelial cells. Biochem Biophys Res Commun 2005;327:700–706.
16. Shen J, Yang X, Xiao WH, et al. Vasohibin is up-regulated by VEGF in the retina and suppresses VEGF receptor 2 and retinal neovascularization. FASEB J 2006;20:723–725.
17. Sato H, Abe T, Wakusawa R, et al. Vitreous levels of vasohibin-1 and vascular endothelial growth factor in patients with proliferative diabetic retinopathy. Diabetologia 2009;52:359–361.
18. Wakusawa R, Abe T, Sato H, et al. Expression of vasohibin, an antiangiogenic factor, in human choroidal neovascular membranes. Am J Ophthalmol 2008;146:235–243.
19. Wakusawa R, Abe T, Sato H, et al. Suppression of choroidal neovascularization by vasohibin-1, vascular endothelium-derived angiogenic inhibitor. Invest Ophthalmol Vis Sci 2011;52:3272–3280.
20. Tobe T, Ortega S, Luna JD, et al. Targeted disruption of the FGF2 gene does not prevent choroidal neovascularization in a murine model. Am J Pathol 1998;153:1641–1646.
21. Heishi T, Hosaka T, Suzuki Y, et al. Endogenous angiogenesis inhibitor vasohibin1 exhibits broad-spectrum antilymphangiogenic activity and suppresses lymph node metastasis. Am J Pathol 2010;176:1950–1958.
22. Krzystolik MG, Afshari MA, Adamis AP, et al. Prevention of experimental choroidal neovascularization with intravitreal anti-vascular endothelial growth factor antibody fragment. Arch Ophthalmol 2002;120:338–346.
23. Miyake Y, Yanagida K, Yagasaki K, et al. Subjective scotometry and recording of local electroretinogram and visual evoked response. System with television monitor of the fundus. Jpn J Ophthalmol 1981;25:439–448.
24. Kondo M, Ueno S, Piao CH, et al. Comparison of focal macular cone ERGs in complete-type congenital stationary night blindness and APB-treated monkeys. Vision Res 2008;48: 273–280.
25. Hogan MJ, Kimura SJ, Thygeson P. Signs and symptoms of uveitis. I. Anterior uveitis. Am J Ophthalmol 1959;47:155–170.
26. Zhang M, Zhang J, Yan M, et al. Recombinant anti-vascular endothelial growth factor fusion protein efficiently suppresses choroidal neovascularization in monkeys. Mol Vision 2008;14:37–49.
27. Husain D, Kim I, Gauthier D, et al. Safety and efficacy of intravitreal injection of ranibizumab in combination with verteporfin PDT on experimental choroidal neovascularization in the monkey. Arch Ophthalmol 2005;123:509–516.
28. Shen WY, Lee SY, Yeo I, et al. Predilection of the macular region to high incidence of choroidal neovascularization after intense laser photocoagulation in the monkey. Arch Ophthalmol 2004;122:353–360.
29. Hosaka T, Kimura H, Heishi T, et al. Vasohibin-1 expression in endothelium of tumor blood vessels regulates angiogenesis. Am J Pathol 2009;175:430–439.
30. Zhou SY, Xie ZL, Xiao O, et al. Inhibition of mouse alkali burn induced-corneal neovascularization by recombinant adenovirus human vasohibin-1. Mol Vision 2010;16:1389–1398.
31. Alon T, Hemo I, Itin A, et al. Vascular endothelial growth factor acts as a survival factor for newly formed retinal vessels and has implications for retinopathy of prematurity. Nat Med 1995;1:1024–1028.

第4章　バイオ・生物製剤への応用に向けた DDS 技術の動向と実用化の可能性

第2節バイオ分野に期待される技術の動向

［1］細胞製剤技術の現状と実用化の課題

東北大学大学院　医学系研究科　助教　博士(工学)　永井展裕

(株)技術情報協会

2013 年 3 月発刊 「DDS製剤の開発・評価と実用化手法」抜刷
231-235 頁

第２節　バイオ分野に期待される技術の動向
［1］　細胞製剤技術の現状と実用化の課題

はじめに

理想的な薬の投与方法は，当然ながら薬物を必要な場所に必要な量だけ必要なときに送り込むことであり，DDSはこれらを達成し薬物治療の効率を向上させることを目標に発展してきた。材料化学の進歩によって，薬剤を持続的に放出（徐放）したり，体内半減期の短い薬剤の寿命を延長したり，薬剤の吸収促進，目的部位へのターゲティングなど，さまざまな方法が可能になってきている。しかし，生体内で起こっている現象は単純ではなく，治療の過程において薬剤が必要な場所や量，種類は常にダイナミックに変化しているはずである。このような生体内の現象に迅速に対応できるDDSは現状では１つしか考えられない。それは「細胞」である。生体の基本単位である細胞は，生体の維持のために必要なところに必要な量だけの分化した細胞を生み，必要なときに必要な量だけ生理活性物質を分泌（徐放）して，生体の諸機能を調節しているのであり，まさにDDSを実践していると言える。従って，生きている細胞を薬として扱う「細胞製剤」は理想的な究極の薬物療法と言っても過言ではない。

細胞を用いる方法として，生体から取り出した細胞を元の機能を維持したまま利用する方法や，個々の病態に対応した生理活性物質の分泌機能を遺伝子導入によって新たに付与した機能化細胞を用いる方法がある。さらに，これらの細胞を目的の場所に投与する方法として，単純に細胞懸濁液を注入する方法や細胞を高分子カプセルで免疫隔離する方法，細胞シート化してから移植する方法などがある。ここではこのような細胞を薬の運び屋として利用する「細胞製剤」の現状を紹介する。

1.　細胞の機能化

細胞をDDSとして用いるとき，移植した細胞が周囲の環境と調和して生理活性物質を持続的に徐放し，標的部位の治癒に積極的に関与することが期待できる。細胞は生きている限り薬（生理活性物質）を徐放し，さらに１種類ではなく複数の薬を環境に応じて徐放するため，１つや２つの薬を包含した従来の材料ベースのDDSよりもはるかに高性能でインテリジェントな効果が期待できる。さらに遺伝子導入によって人工的に新たな機能を付与された細胞を用いる方法も検討されている。ここでは，眼科領域における細胞製剤（細胞治療）を中心に述べてみたい。

1.1　眼科医療における細胞治療

視覚は我々が外から得る情報の約８割を占めると言われている。視覚の中枢となる網膜は，眼球の後ろ側の内壁を覆う薄い膜状の組織であり，視細胞や神経節細胞等の神経細胞から構成され，視覚的な映像（光の情報）を神経信号（電気信号）に変換し，視神経を通して脳中枢へ伝達する働きを持つ。そのため，加齢黄斑変性症や網膜色素変性症などに代表される網膜変性疾患によって網膜に障害が起こると著しい視覚障害を引き起こし，我々の生活の質を著しく低下させる。一部の網膜変性疾患に遺伝子異常が判明している以外，病態については不明なものが多く，一旦発症すると重篤になるものが多く存在し，有効な治療法がないのが現状である。

網膜色素上皮細胞（Retinal pigment epithelium；RPE）は網膜を構成する細胞の中でも，上皮細胞の性質を持つことから神経細胞よりも取扱いが容易であるため，RPEを網膜下に移植して網膜疾患を治療する試みが行われてきた。RPEは視細胞と脈絡膜（血管組織）の間に位置する１層の上皮組織であり，視細胞への酸素や栄養供給など神経網膜の代謝と維持に重要な役割を果たしている。１日に視細胞外節の約10％を貪食し視細胞をリフレッシュしていると言われており，人体の中でも酸素消費量の多い組織である。加齢に伴うRPEの異常によって脈絡膜より新生血管が出現して視細胞を障害する加齢黄斑変性やRPEの遺伝子異常によって発症する網膜色素変性症など難治性網膜疾患と深く関わる組織である。

RPE移植の臨床応用は，1991年以降複数の施設より報告されている。RPE移植は，障害された，もしくは失われ

たRPEの補充として用いられた。過去に報告されたRPE移植は，アイバンクや胎児から得られたRPEが用いられていたが，これら非自己のRPE移植では，移植RPE自体がさまざまな抗原性を持ち，炎症反応や免疫反応を惹起するなど臨床的に拒絶反応が大きいという課題があった。この改善例として，RPEの代用として自己の虹彩色素上皮細胞（IPE）の移植が報告された[1]。この場合も含め，RPEが移植に利用される場合は培養細胞として利用されることがほとんどである。一般的には体外で培養する操作は，生体内における環境と異なるため，RPEがもともと持っている生理的機能（分化機能）を完全に逸脱させた状態となる。培養細胞は微小環境内に移植してあげると，微小環境内で分化した落ち着いた状態になる可能性が指摘されているが，細胞を利用する細胞治療においてはこのような移植後の細胞の挙動が特に重要な問題である。しかし過去の報告を見ると，サルの自己IPEを培養後，懸濁液として網膜下に移植したとき，術後6か月の時点でも網膜下に移植細胞が確認でき，また，移植細胞の増殖反応や拒絶反応は通常の検査方法では見られていない。また，培養細胞を用いる場合，遺伝子導入によって網膜保護作用のある神経保護因子や栄養因子の運搬細胞として利用できる可能性がある。すなわち，各個人にあった効果的な治療を引き出すオーダーメイドの細胞製剤を作ることが可能である。

1.2　遺伝子工学を駆使した細胞治療

培養細胞に遺伝子を組み込む場合，電気刺激を利用して強制的に導入する方法や，リポソームを使用したり，ウィルスベクターに目的遺伝子を組み込んで導入する方法などがある。ベクターに用いるウィルスとして，アデノウィルス，アデノ随伴ウィルス（adeno-associated virus；AAV），レトロウィルス，ヘルペスウィルスなど多数のウィルスが知られている。これらの方法で，上述の網膜神経保護因子の遺伝子を移植細胞に導入し，網膜疾患治療に利用する方法が検討されている。

目的遺伝子を組み込んだプラスミドベクターをリポソームを用いたLipofection法で細胞内に導入し，プラスミドベクターが持つ抗生物質耐性遺伝子を利用して遺伝子導入された細胞を選択する方法がある。もし遺伝子が導入された細胞を特別に選択しない場合，目的遺伝子の発現は極端に低い。選択すると，目的遺伝子を発現する細胞を回収できるが，これには時間がかかり，回収できる細胞も少ないことが多い。そのため，臨床応用を目指した場合，限られた自己の細胞を利用することを考えると，もっと効率の良い方法で遺伝子を導入する必要がある。その点では，ウィルスベクターは導入効率の点で利点がある。

ウィルスベクターにはさまざまな種類があるが，X連鎖遺伝型重症複合免疫不全（X-linked sever combined immunodeficiency：X-SCID）に対するレトロウィルスベクターを用いた遺伝子治療は，大半の患者が免疫能を獲得して通常の生活を送れるようになったが，治療を受けた15名のうち約3年後に3名がTリンパ性白血病を発症し，うち1名が死亡したことが報告された[2]。アデノウィルスベクターではornithine transcarbamylase (OTC) 遺伝子を搭載させたphase Iの毒性試験が1997年に開始されたが，18番目の症例が血液凝固異常と多臓器不全を起こし，4日後に死亡したことが報告された[3]。一方，AAVは病気との関連が知られておらず，染色体に遺伝子を組み込む力はほとんどなく，これまでの臨床応用でも重篤な合併症は報告されていない。AAVにはいくつかの血清型が知られており，それぞれの組織によって感染のしやすさに違いがあることが知られている。網膜に関してはin vivoでは4あるいは5型がRPEや視細胞に導入効率が高いことが判明しており，in vitroでの遺伝子導入については2型が導入効率が高いことが判明した[4]。2型AAVは米国食品医薬品庁（FDA）が臨床応用を認可したAAVであり，米国において12種類の疾患に対して合計30のプロトコールが提唱されている。このうち，パーキンソン病に対しては，3種類の臨床研究が進行している。実際に2型AAVに神経栄養因子である脳由来神経栄養因子（BDNF）遺伝子を組み込んだIPEを網膜下に移植すると，光障害による視細胞死を部分的に抑制することが報告されている[5]。AAVはアデノウィルスに比較して導入効率が悪く発現も遅いが，安全である以外にも長時間発現が持続するなどの利点がある。しかしAAVは細胞内に取り込まれてからは，まだ未知の部分もたくさんあり，今後の研究で導入効率の改善も含めて安全性の証明を検討していく必要がある。